The Islamic University–Gaza
Research and Postgraduate Affairs
Faculty of Science
Master of Physics

الجامعـــــــة الإســـلاميـة– غـزة
شئون البحث العلمي والدراسات العليا
كليـــــــــــة العلـــــــــوم
مـــاجـستيـــر الفيـــــزيـــاء

Improvement of electric and magnetic properties for Li spinel ferrite by divalent Zn^{2+} ions substitution

تأثير أيونات الزنك الثنائية على الخواص الكهربية والمغناطيسية لليثيوم اسبنل فريت

Zana Audah Abu Mosa

Supervised by:

Dr. Hussain Dawoud

Associate Professor of Physics

A thesis submitted to the Faculty of Science as a partial fulfilment of the requirements for the degree of Master of Science in Physics

October/2016

إقـــــرار

أنا الموقع أدناه مقدم الرسالة التي تحمل العنوان:

Improvement of electric and magnetic properties for Li spinel ferrite by divalent Zn^{2+} ions substitution

تأثير أيونات الزنك الثنائية على الخواص الكهربية والمغناطيسية لليثيوم اسبنل فريت

أقر بأن ما اشتملت عليه هذه الرسالة إنما هو نتاج جهدي الخاص، باستثناء ما تمت الإشارة إليه حيثما ورد، وأن هذه الرسالة ككل أو أي جزء منها لم يقدم من قبل الاخرين لنيل درجة أو لقب علمي أو بحثي لدى أي مؤسسة تعليمية أو بحثية أخرى.

Declaration

I understand the nature of plagiarism, and I am aware of the University's policy on this.

The work provided in this thesis, unless otherwise referenced, is the researcher's own work, and has not been submitted by others elsewhere for any other degree or qualification.

Student's name:	زانة عودة محمد أبو موسى	اسم الطالب:
Signature:		التوقيع:
Date:	24 / 1 / 2017	التاريخ:

بسم الله الرحمن الرحيم

الجامعة الإسلامية غزة
The Islamic University of Gaza

مكتب نائب الرئيس للبحث العلمي والدراسات العليا هاتف داخلي 1150

الرقم: ج س غ/35/ Ref:

التاريخ: 14/01/2017 Date:

نتيجة الحكم على أطروحة ماجستير

بناءً على موافقة شئون البحث العلمي والدراسات العليا بالجامعة الإسلامية بغزة على تشكيل لجنة الحكم على أطروحة الباحثة/ زانة عودة محمد ابو موسى لنيل درجة الماجستير في كلية العلوم قسم الفيزياء وموضوعها:

تأثير أيونات الزنك الثنائية على الخواص الكهربية والمغناطيسية لليثيوم اسبنل فريت

Improvement of electric and magnetic properties for Li spinel ferrite by divalent Zn2+ ions substitution

وبعد المناقشة العلنية التي تمت اليوم السبت 16 ربيع الثاني 1438هـ، الموافق 2017/01/14م الساعة الحادية عشر صباحاً بمبني طيبة، اجتمعت لجنة الحكم على الأطروحة والمكونة من:

د. حسين عبد الكريم داوود	مشرفاً و رئيساً	.....
د. سفيان عبد الرحمن تايه	مناقشاً داخلياً	.....
د. مجدي سالم حمادة	مناقشاً خارجياً	.....

وبعد المداولة أوصت اللجنة بمنح الباحثة درجة الماجستير في كلية العلوم/ قسم الفيزياء.

واللجنة إذ تمنحها هذه الدرجة فإنها توصيها بتقوى الله ولزوم طاعته وأن تسخر علمها في خدمة دينها ووطنها.

والله ولي التوفيق،،،

نائب الرئيس لشئون البحث العلمي والدراسات العليا

أ.د. عبدالرؤوف علي المناعمة

Abstract

In the present work magnetic, electric and dielectric properties are investigated for mixed ferrite $Li_{0.5(1-x)}Zn_xFe_{2.5-0.5x}O_4$ (where x=0.0, 0.2, 0.4, 0.6, 0.8 and 1) which are prepared from high purity oxides using standard ceramic technique.

The magnetization (M) is measured at room temperature in the range of the applied field from 148 $A.m^{-1}$ up to 1856 $A.m^{-1}$. The results indicated that the magnetization increased as increasing Zn^{2+} ions for samples of ($x \leq 0.6$) while samples of ($x \geq 0.8$) were considered to be paramagnetic at room temperature which have no magnetization .

DC conductivity (σ) is measured as a function of temperature, the relation between $\ln\sigma$ with temperature indicates that the conductivity increases with increasing the temperature which prove that the samples has a semiconductor behavior. Also the relation between $\ln\sigma T$ and temperature show a change in the slope which is attributed to the change of samples from ferrimagnetic to paramagnetic, Curie point, (T_C). To determine T_C, the inductance was measured as a function of temperature. The inductance increased until T_C, then decreased sharply. T_C is found to decrease with increasing the Zn^{2+} ions.

Dielectric constant (ε), dielectric loss tangent ($\tan\delta$) and AC conductivity (σ_{AC}) have been investigated in the frequency range of $(10^4 - 10^6)Hz$ at room temperature. It is found that the value of ε decreases continuously with increasing the frequency, while σ_{AC} increases with increasing frequency until certain point then it seems to be constant with change of frequency.

Experimental results of $\tan\delta$ show maxima points at certain frequency and these maxima found to be shifted to lower frequency.

الملخص

الهدف من هذا البحث دراسة الخواص المغناطيسية، الكهربائية بالإضافة الى ثابت العازلية والموصلية في حالة التيار المتردد لمركب ليثيوم – زنك فريت حسب الصيغة ($Li_{0.5(1-x)}Zn_xFe_{2.5-0.5x}O_4$) الذي تم تركيبه من أكاسيد عالية النقاء باستخدام الطريقة السيراميكية القياسية، حيث (x= 0.0,0.2,0.4,0.6,0.8 &1).

تم قياس المغنطة (M) عند درجة حرارة الغرفة في مجال مغناطيسي متغير ($A.m^{-1}$ 148 to 1856) واوضحت النتائج ان المغنطة تزداد بزيادة تركيز أيونات الزنك في العينات حتى ($x \leq 0.6$) ، بينما ينعدم التمغنط بزيادة تركيز أيونات الزنك في العينات ($x \geq 0.8$) .

قيست الموصلية الكهربية كدالة في درجة الحرارة ومن العلاقة بين $\ln \sigma$ ودرجة الحرارة تبين انها تزداد بزيادة درجة الحرارة وهذا يحقق ان العينات لها خواص أشباه الموصلات. أيضا العلاقة بين درجة الحرارة و $\ln \sigma T$ أظهرت تغير في ميل المماس، هذا التغير في المماس بسبب انتقال العينة من حالةferrimagnetic الى حالة paramagneticلذا تعبر هذه الدرجة عن درجة كوري .

لقياس درجة كوري تم قياس محاثة الملف كدالة في درجة الحرارة حيث وجد ان المحاثة تزداد باستمرار حتى درجة حرارة معينة عندها يحدث نقص حاد في قيمة معامل الحث وهذه الدرجة هي درجة كوري وقد وجد انها تقل بزيادة تركيز أيونات الزنك.

تم حساب ثابت العزل (ε) والموصلية في حالة التيار المتردد (σ_{AC}) في ترددات ضمن مدى $(10^4 - 10^6) Hz$ في درجة حرارة الغرفة ، وقد وجد ان قيمة ε تقل بزيادة التردد ، بينما تزداد σ_{AC} بزيادة التردد حتى قيمة معينة للتردد ثم تثبت قيمتها باستمرار زيادة التردد.

أوضحت القياسات العملية لثابت الفقد ($\tan\delta$) وجود قيمة عظمى عند قيمة محددة للتردد، ولوحظ أنها تنزاح نحو الترددات الأقل بزيادة تركيز الزنك.

Dedication

This thesis work is, specially, dedicated
To
The continuous source of support, my mother's lovely soul, may Allah rest her in peace and make us abode in paradise
To
My lovely father, may Allah allow him to enjoy health and well being
To
Whom that I've been so lonely without them
My brothers and sisters
And
To all whom have always loved me unconditionally and taught me how to work hard for things that I aspire to achieve.

Acknowledgment

This thesis becomes a reality with the kind support and help of many individuals. I would like to extend my sincere thanks to all of them.

Foremost, I want to offer this success to our GOD Almighty for the wisdom he bestowed upon me, the strength, peace of my mind and good health in order to finish this thesis.

I would like to express my special gratitude and thanks to my adviser ***Dr. Hussain Dawoud****. May Allah bless him, for imparting his knowledge and experiences in this study, which would not have been completed without him.*

I am highly indebted to Physics Department-Faculty of Science in Islamic University of Gaza for their guidance and constant supervision as well as for their support in my study years.

My thanks and appreciation also go to my lovely family, my teachers and friends in all sides of my life for giving me their love, kind wishes, advices and beautifies my life.

Table of Contents

List of Tables

List of Figures

Introduction

Introduction

Materials are called magnetic materials when they are magnetized by a magnetic field. The intensity of the intrinsic magnetization of the magnetic substance M is defined as the magnetic moment μ_{net} per unit volume of the magnetic substance (Rudden and Wilson, 1984). Materials can be classified in terms of their magnetic behaviour, depending on their magnetic susceptibility χ_m values, which change with the applied magnetic field intensity as well as temperature, into one of five groups diamagnetic, paramagnetic, ferromagnetic, antiferromagnetic and ferrimagnetic (Chikazumi, 1964). These groups are illustrated in figure (I).

i. Diamagnetism

Diamagnetism is described for the materials that have a very weak magnetism that results from changes induced in the orbits of electrons in the atoms of a substance by an external magnetic field. They are composed of the atoms which have no net magnetic moment. However, when they expose to an external field, their M acts in the opposite direction of the applied magnetic field H then a negative magnetization is produced and thus; the magnetic susceptibility is negative ($\chi_m < 0$).

ii. Paramagnetism

In paramagnetism, some of the atoms or ions of the substance have a net orbital or spin magnetic moments due to unpaired electrons in partially filled orbitals. In the presence of an external magnetic field, there is a partial alignment of the magnetic moments in the direction of the field resulting in a net small, positive susceptibility ($\chi_m > 0$), when the field is removed the magnetization is zero .

iii. Ferromagnetism

Ferromagnetic materials have some unpaired electrons so their atoms have μ_{net}. Ferromagnetism is described for the materials which their spins are aligned parallel to each other when applied an external magnetic field such that alignment is almost

complete over small regions with a particular overall spin orientation are termed domains. This strong spin alignment leads ferromagnetic materials to have a large, positive susceptibility. They exhibit a strong attraction to magnetic fields and are able to retain their magnetic properties after the external field has been removed. Above a critical temperature, called Curie temperature point T_C, the thermal motion is sufficient to offset the aligning force and the material becomes paramagnetic.

iv. Antiferromagnetism

Antiferromagnetism is described for the materials which have a weak magnetism. It is exhibiting a small, positive magnetic susceptibility. The simplest model structure of these materials consists of two magnetic sublattices with the same magnetic moments, thus; their net magnet moment is zero. The individual magnetic moments on each sublattice are aligned ferromagnetically with antiparallel coupling between the two magnetic sublattices. Above a critical temperature, called Neel's temperature point T_N, thermal energy is sufficient to disorder the individual magnetic moments in antiferromagnetic materials which become paramagnetic.

v. Ferrimagnetism

The structure of the ferrimagnetic materials is composed of more than two magnetic sublattices which are separated by oxygen ions. Therefore, the exchange interactions are mediated by the anions (oxygen, O^{2-} ions). When this happens, the interactions are called indirect or superexchange interactions.

The strongest interactions tend to an antiparallel alignment of the spins between the two sublattices. In these materials, the magnetic moments for the two sublattices are not the same, so the net magnetization of these materials is not zero. Their magnetic moments disappear above Curie temperature point T_C at which the thermal energy randomizes the individual magnetic moments and then these materials become paramagnetic. The color of this material varies from silver gray to black.

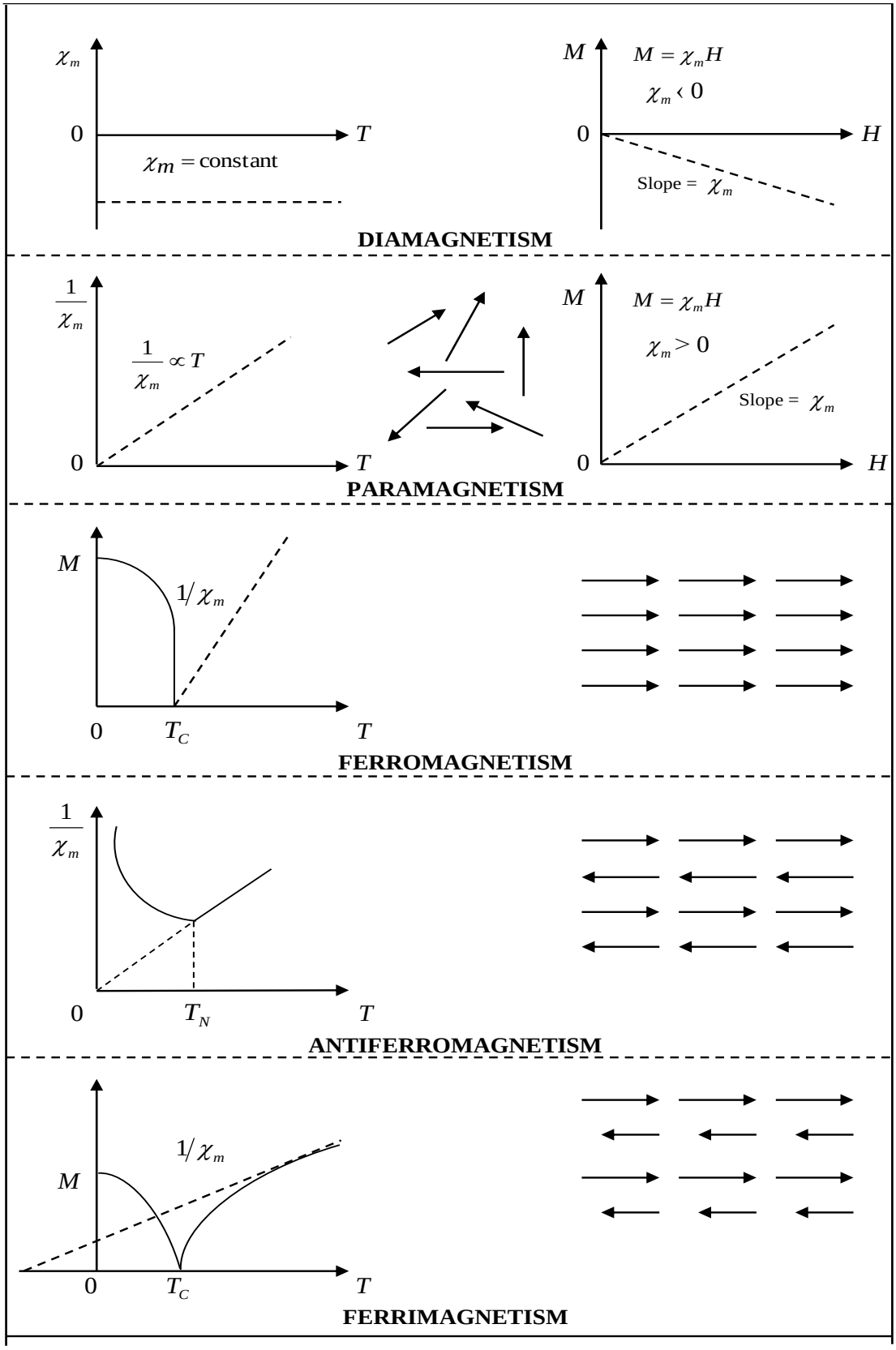

Figure (1): Classification of the magnetic materials.

Classification of Ferrimagnetic Materials

Ferrites are dark brown or gray in appearance and very hard and brittle in physical character. They are prepared by heat-treating the various transition metal oxides or alkaline earth oxides with the ferric oxides (Snoek, 1947). There are many compounds of these materials, which classified in term of either their crystal structure or their applications.

1. According to the crystal structure

There are many compounds of these materials which classified by a term descriptive of their crystal structure. These types are (Morrish, 1965)

i. Ferrimagnetic spinel materials in the form $MeFe_2O_4$, where *Me* is a divalent metal atom of the same type, which may be either magnetic or non-magnetic, such as *Ni, Zn, Cu, Fe, Co, Mn, Mg* or *Cd* , e.g. nickel ferrite $NiFe_2O_4$ and zinc ferrite $ZnFe_2O_4$ also, their combination, e.g. the mixed *Ni- Zn* spinel ferrite.

ii. Hexagonal oxides in the form $MeFe_{12}O_{19}$, where *Me* such as *Ba, Sr, Pb* and their combination, e.g. barium ferrite $BaFe_{12}O_{19}$.

iii. Ferrimagnetic garnet materials in the form $U_3Fe_5O_{12}$, where *U* is replaced by the trivalent rare earth ions, such as *Y, Pm, Sm, Eu, Gd, Tb, Dy, Ho, Er, Tm, Yb* or *Lu*. The rare earth garnets are commonly called RIG's. The commonly example for these materials is yttrium iron garnets YIG's in the form $Y_3Fe_5O_{12}$.

2. According to applications

Ferrimagnetic materials have become available as practical magnetic materials and have a number of important scientific and technological applications. This may be attributed to (Tayal, 1998)

a. They have relativity large saturation magnetization.
b. Their resistivities ranged between $10^2 \Omega.cm$ to $10^{13} \Omega.cm$.
c. They are poor conductors of the electricity, specially, at room temperature.

These properties are valuable in the high frequency application, where the eddy current in the conducting materials poses problems. Ferrimagnetic materials are divided into four groups for applications, which are described in (Dawoud, 1997) as:

i. Hard Ferrites (Permanent Magnets)

Materials used for this application are barium ferrite $BaFe_{12}O_{19}$ and strontium ferrite $SrFe_{12}O_{19}$. These are hexagonal ferrite with a crystal structure of magneto–plumbite $pbFe_{12}O_{19}$. These materials are characterized by a high value of the uniaxial anisotropy field and a high coercive force. In addition, their resistivity is high, typically $10^8 \Omega.cm$. The high coercive force allows these materials to be used as focusing magnets for television tubes, where there are strong demagnetization field. The high resistivity permits their use as permanent magnets where there is additional high frequency magnetic flux without eddy current losses (Smit and Wijn, 1959; Snelling, 1964).

ii. Soft Ferrites

Soft ferrites are ferrimagnetic materials with cubic crystal structure and they are characterized by chemical formula $MO{\cdot}Fe_2O_3$, where M is a transition metal ions like Iron, Nickel, Manganese or Zinc.

The essential requirement is materials with high permeability, low coercive force, low eddy current losses and the ability to operate up to frequencies of $10\,MHz$ with special requirements extending to $1000\,MHz$. The initial permeability of the manganese and the nickel ferrite is rather low, about 250 $(H{\cdot}m^{-1})$ and 10 $(H{\cdot}m^{-1})$, respectively. If these materials are combined with zinc, the anisotropy is lowered and the permeability increases to about 1000 $(H{\cdot}m^{-1})$ for the mixed *Mn-Zn* ferrite and 700 $(H{\cdot}m^{-1})$ for the mixed *Ni-Zn* ferrite. The latter has the higher resistivity and lower losses with higher permeability (Snelling, 1969).

iii. Rectangular Loop Ferrites

Rectangular Loop Ferrites are ferrites which have a rectangular hysteresis loop. This property makes them suitable for use in a magnetic memory core. Ferrite

communities used for this application are the mixed *Mn–Mg* ferrite and the mixed *Li-Ni* ferrite (Albers, 1954; Peloschek, 1963).

iv. Microwave Ferrites

The processing of electromagnetic waves which is done in the frequency range from 1 GHz to 100 GHz are applications of Microwave Ferrites. This processing depends on the interaction of the electromagnetic waves with the processing spin moments in the ferrites. The discussion is restricted to one of the most important of those processes known as Faraday rotation. This is the rotation of the plane of polarization of a plane electromagnetic wave as it travels through the ferrites in the direction of the applied magnetic field. The most application of the Faraday rotation is to use waveguide just as one uses polarizer and analyzer in optics to accept or reject plane polarized wave. The most important microwave ferrites are manganese ferrite, nickel ferrite, cobalt ferrite and the mixed *Ni–Mn* ferrite (Lax and Button, 1962).

Aim of this Study

The aim of this study is to investigate the effect of zinc ions on the magnetic, electric and dielectric properties of mixed ***Li-Zn*** spinel ferrite. AC and DC circuits are used to study the above properties for the mixed ***Li-Zn*** spinel ferrite which was prepared by standard double sintering ceramic technique and have chemical formula of $(Li_{0.5(1-x)}Zn_xFe_{2.5-0.5x}O_4)$ where x is the percentage increment of Zn^{2+} ions in the compound which changes in steps of 0.2 according to $0.0 \leq x \leq 1.0$.

CHAPTER 1

Theoretical Background

CHAPTER 1

Theoretical Background

Ferrites are magnetic oxide materials with semiconducting nature, which are of great technological importance by virtue of their interesting electrical and magnetic properties, so it is important to introduce a theoretical preview about structure, magnetic, electric and dielectric properties of ferrites, which includes in this chapter.

1.1 Structure of Spinel Ferrite Materials

Ferrimagnetic spinel ferrites are the most common compound of the ferrimagnetic materials. The concept of the simplest structure of the ferrimagnetic spinel materials includes two magnetic sublattices. The structure of the ferrite affects the physical properties of these ferrite materials.

1.1.1 Spinel Lattice Structure

The structure of spinel ferrites is derived from that of the mineral spinel $MgAl_2O_4$. The spinel structure, which have a formula AB_2O_4, is usually described as a cubic close-packed (***CCP***) array of oxygen atoms with the A and B cations occupying one eighth of the tetrahedral sites and one half of the octahedral sites. The occupancy of the interstitial sites results in a face centered cubic (***FCC***) unit cell which is 2×2×2 times that of the basic ***CCP*** oxygen array, therefore the unit cell contents are $A_8B_{16}O_{32}$ (Putnis, 1992). As shown in figure (1.1a), ***A*** ions fill the tetrahedral interstices, i.e. T_d sites, and ***B*** ions fill the octahedral interstices, i.e. O_h sites, of the cations packing (Gorter, 1954). Figure (1.1a), also, shows two units of AB_2O_4 in a quarter of the unit cell. The lattice constant "*a*" for these materials varies with the compositions, it is about $8.5A^O$. Figure (1.1 b) shows an isolated O^{2-} ion with its nearest neighbors of the ***A*** and ***B*** ions (Dawoud, 1997). Oxygen atoms have an ionic radius of about 1.32 A°, this is larger than of the ionic radius of the metal ions, which varies between 0.6 A° to 0.8 A° (Chikazumi, 1964). Spinel lattice distribution is affected by many factors like electrons configuration, electrostatic energy and ionic radii, this tends that, the metal ions occupy the interstitial

position sites of the spinel lattice structure, which can be classified into two groups (Dawoud, 1997)

i. The T_d sites interstices are filled by the ***A*** ions, which have the ionic charge **p** and surround by four $\mathbf{O^{2-}}$ ions. They are represented by the bracket ( ).

ii. The O_h sites interstices are filled by the ***B*** ions, which have the ionic charge **q** and surround by six $\mathbf{O^{2-}}$ ions. They are represented by the bracket { }.

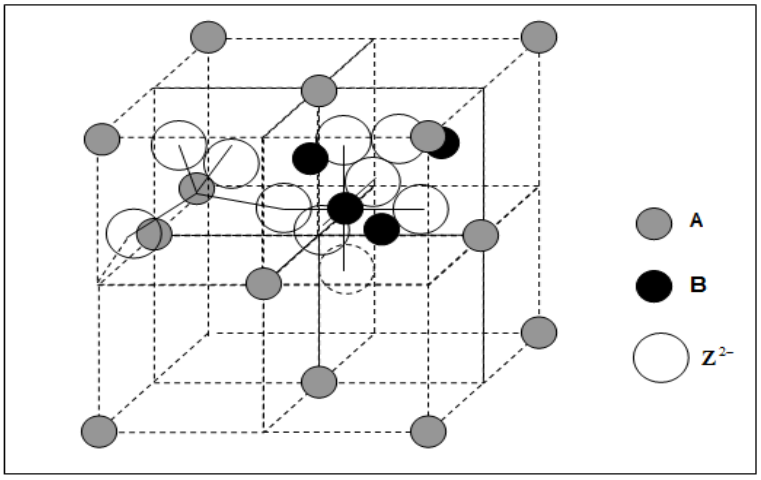

Figure (1.1 a): Two octants of the unit cell of the spinel lattice structure *A* ions are at T_d sites and *B* ions are at O_h sites of the $\mathbf{Z}^{2-}$ anions packing.

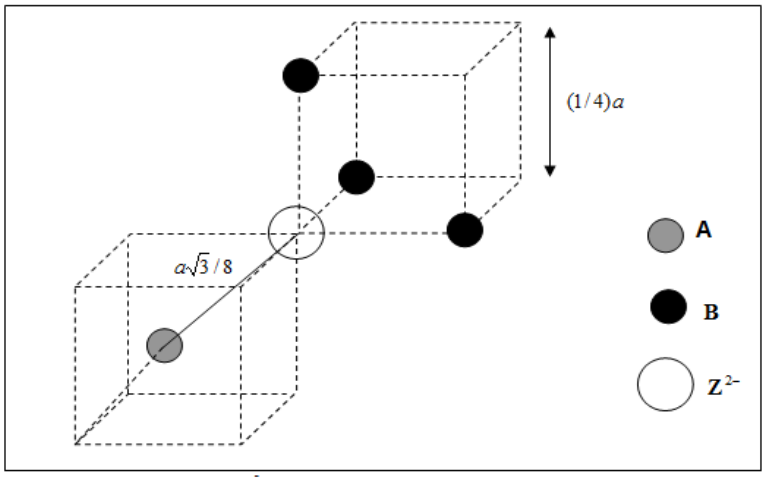

Figure (1.1 b): An anion $\mathbf{Z}^{2-}$ in the spinel lattice structure with it's nearest cations neighbours.

In the spinel lattice structure, the anions have a negative charge equal (-8), which comes from the four depend on the ***A*** and the ***B*** ions, while the cubic closed- packed lattice of the material is the same. The various possibilities of **p** and **q** values were listed in Table (1.1) (Verwey and Helimann, 1947).

Table (1.1): Various possibilities of the ionic charge distribution of the cations of the spinel lattice structure.

Ionic charge value		Ionic Charge Distribution of Spinel Lattice	Type of Spinel Materials
P	**q**		
2	3	$(\mathbf{A}_1^{2+})\{\mathbf{B}_2^{3+}\}\mathbf{Z}_4^{2-}$	(2-3) Spinel Type.
4	2	$(\mathbf{A}_1^{4+})\{\mathbf{B}_2^{2+}\}\mathbf{Z}_4^{2-}$	(4-2) Spinel Type.
3	5/2	$(\mathbf{A}_1^{3+})\{\mathbf{B}_2^{(5/2)+}\}\mathbf{Z}_4^{2-}$	(3-5/2) Spinel Type.
6	1	$(\mathbf{A}_1^{6+})\{\mathbf{B}_2^{1+}\}\mathbf{Z}_4^{2-}$	(6-1) Spinel Type.

The common type of the spinel lattice structure is (2-3) spinel type, which have the highest electrostatic stability in the normal cations arrangement (Verwey, Deboer and Vansanten, 1948). Hence, the ***A*** and the ***B*** ions have various distributions, this makes a change in some of the physical properties of these materials.

The simplest example for the ferrimagnetic spinel materials are the spinel iron, e.g. magnetite (magnetic oxide of iron) in the form ($Fe_1^{2+}Fe_2^{3+}O_4^{2-}$). Several mixed spinel ferrites can be produced by adding different oxides to the iron oxides, which give useful physical properties for several applications.

1.1.2 Types of Spinel Lattice Structure

The distribution of the metal ions at T_d and O_h sites is very important to understand the physical properties of the ferrimagnetic materials. More than one type of this distribution is found at the two sites for the materials in the form $MeFe_2O_4$.

These types are described by (Dawoud, 1997) as:

i. Normal Spinel Structure: In this type, all the Me^{2+} divalent metal ions are found on the T_d sites and the Fe^{3+} trivalent iron ions appear only on the O_h sites. The formula of this type is found in the form

$$(Me^{2+})\{Fe_2^{3+}\}O_4^{2-}$$

ii. Inverse Spinel Structure: In this type, all the Me^{2+} divalent metal ions are found on the O_h sites. and Fe^{3+} trivalent iron ions are distributed in equal numbers over T_d and O_h sites. The formula of this type is found in the form

$$(Fe^{3+})\{Me^{2+}Fe^{3+}\}O_4^{2-}$$

iii. Intermediate Spinel Structure: In the intermediate spinel structure the divalent metal ions Me^{2+} and the trivalent iron ions Fe^{3+} are distributed on the T_d and O_h sites. The formula of this type is found in the form

$$(\ Fe_x^{3+}Me_{1-x}^{2+})\ \{\ Me_x^{2+}Fe_{1-x}^{3+}\}\ O_4^{2-}$$

1.2 Magnetic Properties of the Ferrimagnetic Materials

The ferrites are ionic compounds, and their magnetic properties are due to the magnetic ions they contain. Since it is difficult to calculate the orbital magnetic moments in the ionic crystal, the intensity of the intrinsic magnetization of the ferrimagnetic spinel materials can be explained according to the spins distribution of the magnetic ions at the T_d sites and the magnetic ions at the O_h sites that shown in figure (1.2) (Dawoud, 1997; Lovell, Avery and Vernon, 1976) . It arises usually from the spin magnetic moments of the unfilled shells 3d, for the transition elements, where the superexchange interaction between the sublattices and the six-2p oxygen electrons occurred. Such that an alignment of spins should be expected from the nature of the superexchange interactions. The superexchange interactions between the two cations; via an intermediate O^{2+} ions are greatest, if the three ions are colinear and their separations are not too large.

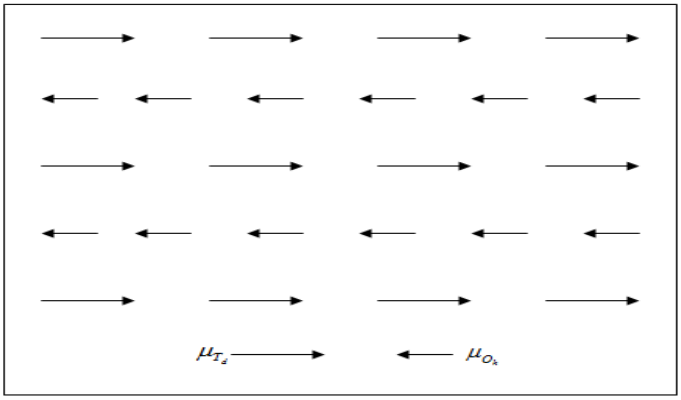

Figure (1.2): Spins distribution at T_d and O_h sites.

The ions arrangement in the spinel lattice is likely to be most important as is shown in figure (1.3 a throught e) (Morrish, 1965; Smit and Wijn, 1959). For the situation depicted in figure (1.3 a) both the angle φ and the distance between the ion cores are favorable for superexchange interactions. For all the other cases, either the angle of figure (1.3 c) or the distance of figures (1.3 b and 1.3 d), or both figure (1.3 e) are unfavorable. The conclusion is that the interactions between the sublattices are stronger than those within them. Further, these interactions between the ions within the T_d sites are the weakest of all. This result thus, supports the assumption that the sublattices magnetizations are antiparallel.

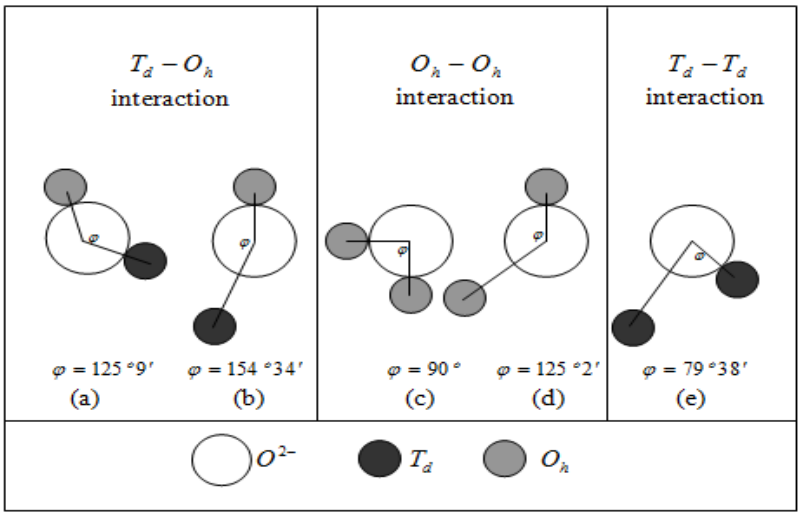

Figure (1.3): Super exchange interactions between the anions, O^{2-} ions, and the cations, the T_d and the O_h sites.

1.2.1 Magnetization Process of the Ferrimagnetic Materials

The relation between the flux density, B **(**$wb.m^{-2}$), and the applied field intensity, H **(**$A.m^{-1}$), is not linear for ferrimagnetic materials. It depends on the previous magnetic history, mechanical and thermal properties as well as on the treatment of the materials being tested. When H is applied to the ferrimagnetic substance, the resulting B is composed of the free space and the contribution of the aligned domains. The B can be expressed as following (Crangle, 1991)

$$B = \mu_o\ (H + M) \tag{1.1}$$

where

$\mu_o = 4\pi \times 10^{-7}$ $(wb.m/A)$ is the permeability of the free space.

H $(A.m^{-1})$ is the applied magnetic field intensity.

M **(**$A.m^{-1}$) is the intensity of the intrinsic magnetization of the substance.

Equation (1.1) is exact for all substances including ferrimagnetic materials. It is useful to define M by

$$M = \chi_m H \tag{1.2}$$

where χ_m is a dimensionless quantity which is known as the magnetic susceptibility of the material. Substituting equation (1.2) into equation (1.1), this gives

$$B = \mu_o(1+\chi_m)H$$

$$B = \mu_o\mu_r H = \mu H \tag{1.3}$$

where $\mu_r = 1+\chi_m$ is a new dimensionless quantity which is known the relative permeability and μ ($\mu = \mu_o\mu_r$) is the permeability of the substance.

1.2.2 Ferrimagnetic Domains

All ferrimagnetic materials consist of many microscopic regions called Wiess domains (Ferroxcube, 2002), within them all the magnetic moments are aligned in the same direction. These domains have a volume of about 10^{-12} m^3 to 10^{-8} m^3 and contain 10^{17} to 10^{21}atoms (Serway, 1996). The magnetizations within the domains are called the

intrinsic magnetization per unit mass at temperature T and its value at zero H is the spontaneous magnetization. The saturation magnetization (M_s) is the value of the spontaneous magnetization at zero temperature (Crangle, 1991).

In unmagnetized sample of the ferrimagnetic substance, the domains are randomly oriented; therefore, μ_{net} is zero. As shown in figure (1.4 a), the domains are randomly oriented since there is no any an external magnetic field applied to the unmagnetized sample. When H increases, the domains become more aligned in the direction of H by rotating slightly until all of them are nearly aligned as shown in figure (1.4 d). At this state, the saturation condition corresponds to the state where all domains are in the same direction parallel to H, which results in a magnetized sample (Ferroxcube, 2002).

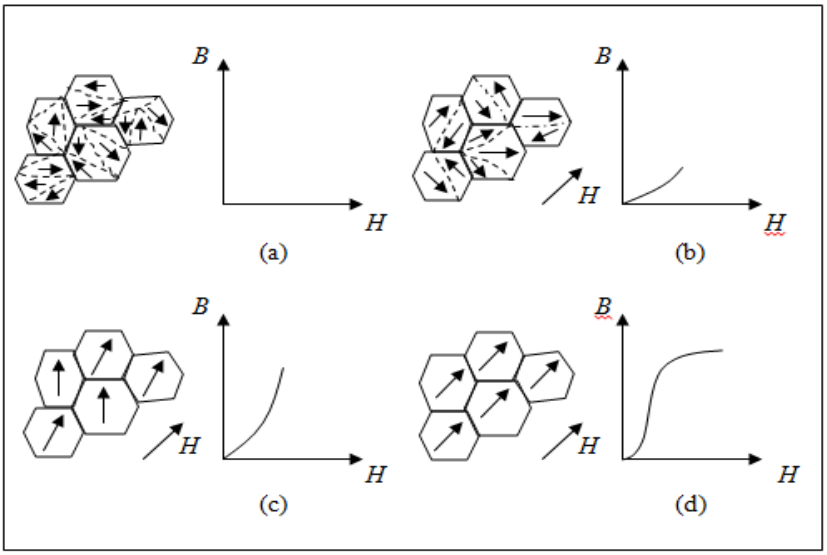

Figure (1.4): Alignment of Wiess domains.

1.2.3 Molecular Field Theory of the Ferrimagnetic Materials

Neel (Neel, 1948) considered that, a ferrimagnetic crystal lattice could be divided into two magnetic sublattices or groups, i.e. T_d and O_h sites, in the spinel lattice structure, where their magnetic moments are not equal, so that, a net magnetic moment is found. This happens either because they are made from elements in different ionic state, e.g. Fe^{2+} and Fe^{3+}, or from different elements in the same or different ionic states,

e.g. Co^{2+} and Fe^{3+} (Morrish, 1965). This can be explained by the molecular field theory of the ferrimagnetic materials.

In order to analyze the ferrimagnetic effects, one needs to calculate the molecular field on each site of a particular atom that caused by an external source and the magnetic atoms in the medium. The molecular magnetization field H_{mT} and H_{mO} of the T_d and the O_h sites, respectively, may be written in the scalar form (Sattar, El-Sayed and Agami, 2007)

$$\begin{pmatrix} H_{mT} \\ H_{mO} \end{pmatrix} = -\begin{pmatrix} N_{TT} & N_{TO} \\ N_{OT} & N_{OO} \end{pmatrix}\begin{pmatrix} M_T \\ M_O \end{pmatrix}$$

(1.4)

where

H_{mT} is the molecular magnetization field acting on the ions at T_d sites.

H_{mO} is the molecular magnetization field acting on the ions at O_h sites.

M_T is the intensity of the intrinsic magnetization within the T_d sites.

M_O is the intensity of the intrinsic magnetization within the O_h sites.

N_{TO} and N_{OT} are the molecular magnetization field constant for the next nearest neighbor interactions between the T_d sites and the O_h sites.

N_{TT} and N_{OO} are the molecular magnetization field constant for the next neighbor interactions within the T_d sites and the O_h sites, respectively.

Here, $N_{TO} > 0$, since the interactions between the two sublattices are antiferromagnetic. The other molecular field constants, N_{TT} and N_{OO}, may in principle be positive or negative, but they are apparent positive for the great majority of the ferrimagnetic materials. They are, also, small compared to N_{TO}, where at equilibrium $N_{TO} = N_{OT}$,

however, $N_{TT} \neq N_{OO}$ since the sublattices are crystallographically inequivalent. Therefore, $M_T \neq M_O$. If an external magnetic field H is, also, applied to the ferrimagnetic substance the total magnetic fields H_T and H_O on the atoms at the T_d and the O_h sublattices, respectively, are

$$\begin{pmatrix} H_T \\ H_O \end{pmatrix} = H + \begin{pmatrix} H_{mT} \\ H_{mO} \end{pmatrix} \tag{1.5}$$

Substituting equation (1.4) into equation (1.5), this gives

$$\begin{pmatrix} H_T \\ H_O \end{pmatrix} = H + \begin{pmatrix} N_{TT} & N_{TO} \\ N_{OT} & N_{OO} \end{pmatrix} \begin{pmatrix} M_T \\ M_O \end{pmatrix} \tag{1.6}$$

The magnetization field constants N_{TT} and N_{OO}, can be expressed in terms of N_{TO}. Let $N_{TT} = \alpha N_{TO}$ and $N_{OO} = \beta N_{TO}$ with $N_{TO} = N_{OT}$. This notation is of some value for temperature region in which the system is ordered (Morrish, 1965). Therefore, equation (1.6) becomes as the following.

$$\begin{pmatrix} H_T \\ H_O \end{pmatrix} = H - \begin{pmatrix} \alpha N_{TO} & N_{TO} \\ N_{OT} & \beta N_{TO} \end{pmatrix} \begin{pmatrix} M_T \\ M_O \end{pmatrix}$$

$$\begin{pmatrix} H_T \\ H_O \end{pmatrix} = H - N_{TO} \begin{pmatrix} \alpha & 1 \\ 1 & \beta \end{pmatrix} \begin{pmatrix} M_T \\ M_O \end{pmatrix} \tag{1.7}$$

Solving for the following matrix

$$\begin{pmatrix} \alpha & 1 \\ 1 & \beta \end{pmatrix} \Rightarrow \begin{Bmatrix} = 0 \\ \neq 0 \end{Bmatrix} \tag{1.8}$$

According to the equation (1.8), there are two solutions for the above matrix. In the case of zero value the substance may be considered as the antiferromagnetic substance but, in the other case, it may be considered as the ferrimagnetic substance.

The intensity of the intrinsic magnetizations M_T and M_O of each sublattice at thermal equilibrium depends on the spin quantum number S_m for the ions within the sublattices as well as temperature. Therefore, M_T is given by (Morrish, 1965)

$$M_T = \sum_i N_i g_i \mu_B S_{mi} B_{S_{mi}}(x_T) \tag{1.9}$$

where

$$x_T = \frac{S_{mi} g_i \mu_B H_T}{kT} \tag{1.10}$$

and $B_{S_{mi}}(x_T)$ is called **Brillouin** function, which is written in the form (Anton, 1984)

$$B_{S_{mi}}(x_T) = \frac{2S_{mi}+1}{2S_{mi}} \coth\left(\frac{2S_{mi}+1}{2S_{mi}} x_T\right) - \frac{1}{2S_{mi}} \coth\left(\frac{x_T}{2S_{mi}}\right) \tag{1.11}$$

Likewise, M_O is given by

$$M_O = \sum_j N_j g_j \mu_B S_{mj} B_{S_{mj}}(x_O) \tag{1.12}$$

and

$$x_O = \frac{S_{mj} g_j \mu_B H_O}{kT} \tag{1.13}$$

where

N_i and N_j	are the number of the atoms, i.e. the magnetic ions, per unit volume at the T_d and the O_h sublattices, respectively.
S_{mi} and S_{mj}	are the spin quantum number for the atoms at the T_d and the O_h sublattices, respectively.
g_i and g_j	are the lande' splitting factor, which is approximately equal to 2.0003 for the free electron.
μ_B	is the Bohr magneton and *k* is the Boltzmann's constant.

The conclusion is that, the magnetization of each sublattice depends on temperature as well as the applied magnetic field. For a very small-applied magnetic field, the spontaneous magnetization of the ferrimagnetic materials changes with increasing of temperature as shown in Figure (1.5) (Crangle, 1991).

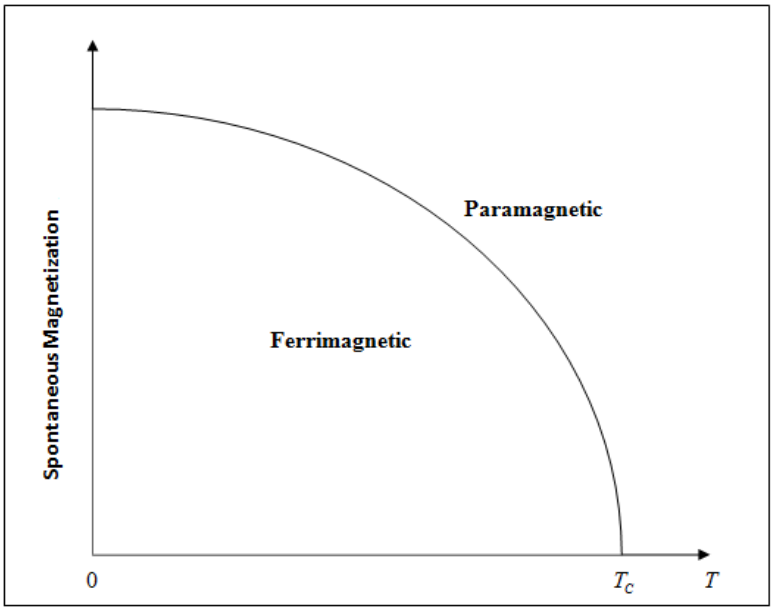

Figure (1.5): Spontaneous magnetization of the ferrimagnetic materials as a function of the absolute temperature

This curve closely follows a mathematical expression known as a Brillouin function. When this decreasing reaches a critical temperature called Curie temperature point T_C or the paramagnetic region, the spontaneous magnetization of the ferrimagnetism vanishes. The temperature dependence of the ferrimagnetic materials below T_C is important. This is because T_C has an effect on the magnetic, the electric and the dielectric properties. It, also, determine the applications of the ferrimagnetic materials.

When the temperature equal T_C , where *H* is constant and very small, therefore, x_T and x_O become very small quantities. The approximation of the Brillouin function may be written as (Anton, 1984)

$$B_{S_m}(x) = \frac{(S_m + 1)}{3S_m} x - (\frac{(S_m + 1)}{3S_m} \frac{2{S_m}^2 + 2S_m + 1}{30{S_m}^2}) x^3 \tag{1.14}$$

If $x << 1$, the second term on the right hand side of the equation (1.14) will decrease to an infinitely small value, so it will be neglected. Therefore, M_T and M_O are given by (Morrish, 1965)

$$M_T = \sum_i N_i g_i \mu_B S_{mi} \left(\frac{S_{mi} + 1}{3S_{mi}} \right) x_T \tag{1.15}$$

and

$$M_O = \sum_j N_j g_j \mu_B S_{mj} \left(\frac{S_{mj} + 1}{3S_{mj}} \right) x_O \tag{1.16}$$

Substituting equation (1.10) into equation (1.15), thus; the M_T is given by

$$M_T = \frac{C_T}{T} H_T \tag{1.17}$$

Similarly substituting equation (1.13) into equation (1.16) thus; the M_O is given by

$$M_O = \frac{C_O}{T} H_O \tag{1.18}$$

$$C_{T,O} = \sum_{i,j} N_{i,j} \frac{g_{i,j}^2 \mu_B^2 S_{mi,mj} \left(S_{mi,mj} + 1 \right)}{3k} \tag{1.19}$$

To evaluate the magnetic susceptibility χ_m, that is given by

$$\chi_m = \frac{M}{H} \tag{1.20}$$

where the intensity of the intrinsic magnetization of the magnetic materials may be written in the scalar form *M*, which is given by (Dawoud, 1997; Morrish, 1965)

$$M = M_T + M_O \tag{1.21}$$

This implies that,

$$\chi_m = \frac{M_T + M_O}{H} \tag{1.22}$$

Upon substituting equation (1.17) and equation (1.18) into equation (1.22), thus;

$$\frac{1}{\chi_m} = \frac{T}{C} + \frac{1}{\chi_{mo}} - \frac{\delta}{T - \theta'} \tag{1.23}$$

where *C* is the **Curie** constant which is given by $C = C_T + C_O$, and

$$\frac{1}{\chi_{mo}} = -\frac{1}{C}(C_T^2 N_{TT} + C_O^2 N_{OO} + 2C_T C_O N_{TO})$$

$$\delta = -\frac{C_T C_O}{C^3}\{C_T^2(N_{TT} - N_{TO})^2 + C_O^2(N_{OO} - N_{TO})^2 \ - 2C_T C_O[N_{TO}^2 - (N_{TT} + N_{OO})N_{TO} + N_{TT}N_{OO}]\}$$

$$\theta' = -\frac{C_T C_O}{C}(N_{TT} + N_{OO} - 2N_{TO})$$

Ferrimagnetic materials become paramagnetic above Curie temperature point and in this region the graphical representation of the equation (1.23) is a hyperbola as shown in figure (1.6). In the limit at large temperature, i.e.$T \to \infty$, the last term in equation (1.23) disappears, but the asymptote equation (1.24) is given by the remains terms

$$\frac{1}{\chi_m} = \frac{T}{C} + \frac{1}{\chi_{mo}} \tag{1.24}$$

If γ is defined as the *T*-intercept found by extrapolation of the line, then, $\gamma = -C/\chi_{mo}$, Neel's called this asymptotic Curie temperature point. Therefore, the equation (1.24) becomes

$$\chi_m = \frac{C}{T - \gamma} \tag{1.25}$$

This means that, when temperature is equal to Curie temperature point the ferrimagnetic substance will be considered as the paramagnetic substance.

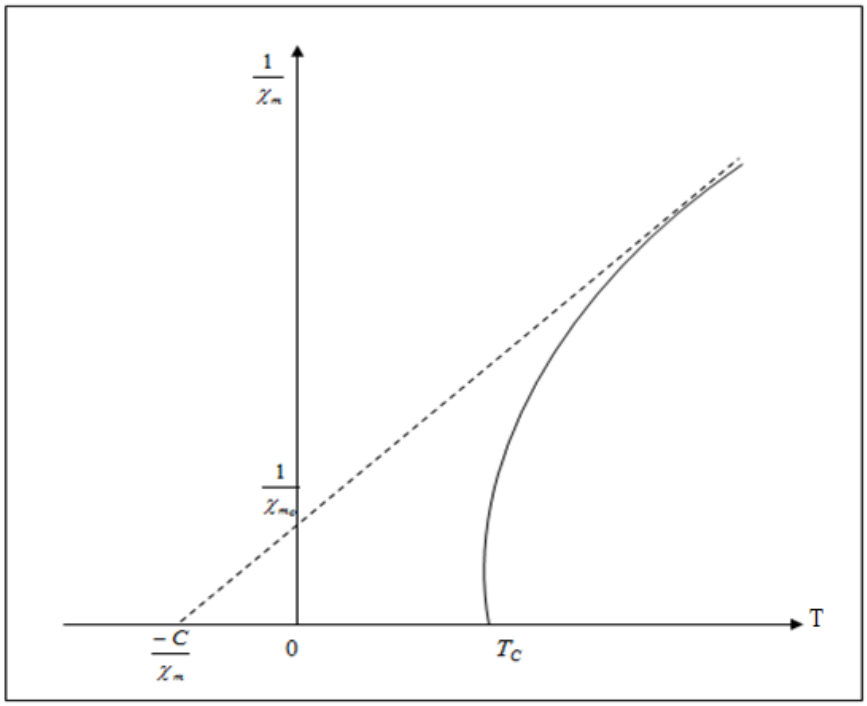

Figure (1.6): Inverse magnetic susceptibility of the ferrimagnetic materials above the T_C according to the molecular field theory.

1.3 Electric Properties of the Ferrimagnetic Materials

The electrical properties of ferrites are sensitive to preparation method, sintering temperature, sintering time, rate of heating and rate of cooling (Kulkarani, Todhar and Vaingankar, 1986; Rezlesus and Rezlesus, 1974). The study of electrical conductivity produces valuable information on behavior of free and localized electric charge carried in the sample.

1.3.1 Conductivity of the Ferrimagnetic Materials

The conductivity σ of the ferrimagnetic materials depends on temperature and the measuring frequency of the applied field. This is controlled by the cations concentration on the sites of the spinel lattice structure (Patil, Sawant, Patil and Patil, 1994). Therefore, their conductivity can be expressed according to (Chikazumi, 1964)

$$\sigma = \sigma_o e^{-E_a/kT} \tag{1.26}$$

where $\sigma_\circ$ is temperature dependent constant, E_a represents the activation energy, which is the energy required to release an electron from the ion for a jump to the neighboring ion, so that, giving rise the electric conductivity, and K is Boltzmann constant .

Almost all of the known ferrimagnetic materials are poor conductors of electricity, the resistivity ρ of the ferrites at room temperature varies from $10^{-2}\Omega.cm$ to $10^{11}\Omega.cm$, which depends on the chemical composition (Smit and Wijn, 1959).

1.3.2 Conduction Mechanism in the Ferrimagnetic Materials

The conduction mechanism in the ferrimagnetic materials is different and much less understood in comparison with the elements in-group IV semiconductors such silicon and germanium (Patil et al, 1994).

In the ferrimagnetic materials, the concentration of the charge carriers is larger than semiconductor materials (Verwey, Deboer and Vansanten, 1948). The nature of charge carriers in ferrimagnetic oxides have been the subject of many experimental and theoretical studies, however, until now no conclusive theory has been formulated for conduction mechanism in these materials (Mazen, Ghani and Ashotr, 1985).

The conduction mechanism is attributed to the hopping of the electrons between $\boldsymbol{Fe^{2+}}$ ions and $\boldsymbol{Fe^{3+}}$ ions. The $\boldsymbol{Fe^{2+}}$ ions are considered the donors that contain extra electron, which will jump to the adjacent $\boldsymbol{Fe^{3+}}$ ions easily and will constitute the electrons conduction. The oxidation of the divalent iron ions reduces donor content in the material such that, the electric resistivity is increased (Cheng, 1984).

The conductivity in ferrites associates with the presence of the ions for the element in more than one valence state; these ions are distributed over the crystallographically inequivalent sites (Patil et al, 1994). The conduction mechanism of the ferrites depends on temperature. Therefore, the conductivity will be described as in equation (1-26).

The detailed behavior of the complex compounds such that ferrimagnetic materials are not well understood. In general, the conduction at lower temperature is due to hopping

electron between $Fe^{2+} \Leftrightarrow Fe^{3+}$ ions (Uitert, 1956), whereas at a higher temperature is due to the hopping polarons (Klinger, 1975; Klinger, 1977)

Since the mobile carriers have spin magnetic moments, they are strongly influenced in their motion by the direction of spins on neighboring sites. And they can polarize the lattice sites. Therefore, the combination of the mobile carriers and lattice polarization is known as a magnetic polaron (Lovell, Avery and Vernon, 1976).

It is found that, the neighboring spins forming a ”magnetic polaron”. However, the motion of the polaron is always characterized by a large effective massed and low mobility. If the polarization is much localized the polaron is called small polaron and usually moves bythermal activation. At high temperatures, the electron moves from site to site by thermally activated hopping; at low temperature the electron tunnels slowly through the crystal (Kittel, 1976). In the neighborhood of T_C thermal vibrations are disordering spins. The motion of a charge carrier may be strongly influenced by the scattering produced by the disordered spins.

1.4 Dielectric Properties of the Ferrimagnetic Materials

The polycrystalline ferrites, which have many applications at microwave frequencies are very good dielectric materials. The dielectric properties of the ferrites depend on several factors including (Ravinder and Latha, 1999) the method of preparation, Sintering temperature, Sintering atmosphere, Frequency applied and chemical composition.

When a ferrite powder is sintered under gradually reducing conduction the divalent iron ions are formed in the bulk. This leads to high conductivity ferrite grains, which has a very high dielectric constant $\boldsymbol{\varepsilon}$ (Eatah, Ghani and Faramawy, 1988). The electrons exchange interaction between the $\boldsymbol{Fe^{2+}}$ ions and the $\boldsymbol{Fe^{3+}}$ ions result in a local displacement of the electrons in the direction of the electric field. This determines the polarization of the ferrites. Therefore, the $\boldsymbol{Fe^{2+}}$ ions play a dominant role in the mechanisms of the conductivity and the electric polarization. The concentration of the

Fe^{2+}ions depends on sintering temperature and sintering atmosphere (Reddy and Reddy, 1991).

1.4.1 Dielectric Theory of the Ferrimagnetic Materials

In order to obtain quantitative information about the behavior of the ferrite, precise impedance measurements were carried out with disks of several compositios. In general, the dielectric constant is roughly inversely proportional to the square root of the resistivity. Both quantities depend on the measuring frequency of the applied field (Smit and Wijn, 1959).

Maxwell-Wagner two layer model was used to explain the high apparent permittivity at low frequency dispersion in polycrystalline ferrites (Koop, 1951; Moitgen and Angew, 1952), A well-conducting bulk material with conductivity σ_1, permittivity ε_1 and thickness d_1 is separated by poorly conducting layers with conductivity σ_2 , permittivity ε_2 and thickness d_2 . From the equivalent layer model of figure (1.7), the permittivity ε and the effective conductivity σ can be obtained as a function of the frequency.

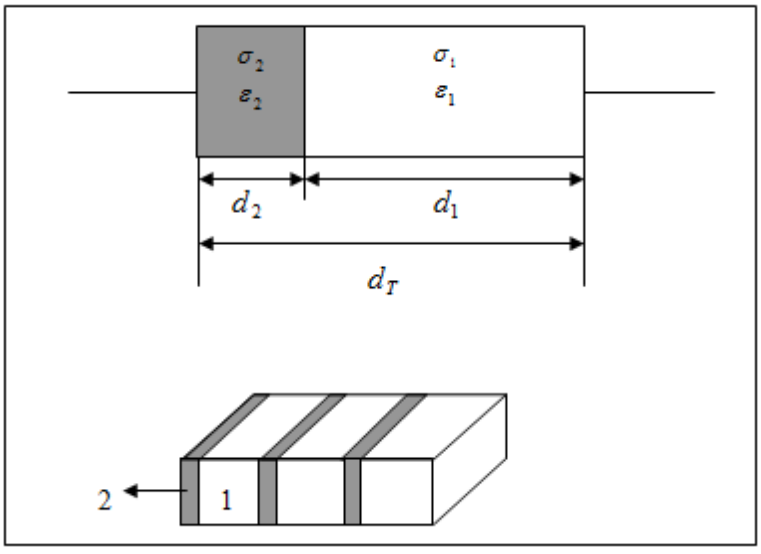

Figure (1.7): Equivalent layers model of the Maxwell-Wagner theory.

The dispersion formula for the permittivity ε and the conductivity σ can be described by the terms in the form (Dawoud, 1997; Smit and Wijn, 1959)

$$\sigma = \sigma_{h\nu} + \frac{\sigma_{l\nu} - \sigma_{h\nu}}{1 + (\omega\tau_{\sigma})^2} \tag{1.27}$$

$$\varepsilon = \varepsilon_{h\nu} + \frac{\varepsilon_{l\nu} - \varepsilon_{h\nu}}{1 + (\omega\tau_{\varepsilon})^2} \tag{1.28}$$

where, the indices $l\nu$ and $h\nu$ indicate the limiting values at low and high frequency, respectively. The relaxation time τ is a characteristic time constant of ferrites. Thus; the relaxation frequency $\omega \propto 1/\tau$ for the different materials appears to be approximate proportional to the low-frequency value of the dielectric constant (Smit and Wijn, 1959).

Referring to the figure (1.7), suppose that z is defined by the ratio between the thickness of the grains boundary layer (d_2) and the thickness of the ferrite grains layer (d_1), which is written by

$$z = \frac{d_2}{d_1} \tag{1.29}$$

Suppose that $z << 1$, then the parameters $\sigma_{h\nu}, \sigma_{l\nu}$ and τ_{σ} in the equation (1.27) can be given as the follows (Koop, 1951)

$$\sigma_{h\nu} = \frac{\sigma_1\sigma_2(\varepsilon_1 + z\varepsilon_2)^2}{\sigma_1\varepsilon_1^2 + z\sigma_2\varepsilon_2^2} \tag{1.30}$$

$$\sigma_{l\nu} = z\sigma_1 + \sigma_2 \tag{1.31}$$

$$\tau_{\sigma} = \varepsilon_o\left(\frac{\sigma_1\sigma_2(\sigma_1\varepsilon_1^2 + z\sigma_2\varepsilon_2^2)}{z\sigma_1 + \sigma_2}\right)^{\frac{1}{2}} \tag{1.32}$$

In the same way, the parameters $\varepsilon_{h\nu}, \varepsilon_{l\nu}$ and τ_{ε} in the equation (1-29) can be given as the follows

$$\varepsilon_{h\nu} = \frac{\varepsilon_1\varepsilon_2}{\varepsilon_1 + z\varepsilon_2} \tag{1.33}$$

$$\varepsilon_{l\nu} = \frac{\sigma_2^2\varepsilon_2 + z\sigma_1^2\varepsilon_1}{(z\sigma_1 + \sigma_2)^2} \tag{1.34}$$

$$\tau_{\varepsilon} = \varepsilon_o \left(\frac{\sigma_1 \sigma_2 (\varepsilon_1 + z\varepsilon_2)}{z\sigma_1 + \sigma_2} \right) \tag{1.35}$$

It can be found that, the relation between τ_{ε} and τ_{σ} is given by (Koop, 1951)

$$\tau_{\varepsilon} = \left(\frac{\sigma_{h\nu}}{\sigma_{l\nu}} \right)^{1/2} \tau_{\sigma} \tag{1.36}$$

This phenomenological theory is generally used to describe the dielectric relaxation in the ferrites at constant temperature mostly room temperature. The idea of this investigation was to find out whether the inhomogeneity model holds for the variation of temperature.

1.4.2 Dielectric Loss Tangent

A study of the dielectric properties of the ferrimagnetic materials is interesting and has practical value. When an *AC* voltage is applied to a circuit containing a capacitor, only the displacement current I_D or the capacitive current I_C will flow across the capacitor if the material filling the capacitor is a perfect dielectric. In that case no electromagnetic energy will be lost in the capacitor. Since perfect dielectrics hardly exist, there is usually a resistive current, $I_{Res.} = V_{in} / R_{in}$ running through the material, as well as the displacement current. The resistive current is responsible for the energy losses in the dielectric materials. The resistive component of the total current is in phase with the voltage applied to the capacitor (Nwanje, 1980).

Let the applied voltage due to the capacitor V_C in an *AC* voltage circuit containing a capacitor is given by

$$V_C = V_T e^{i\omega t} \tag{1.37}$$

then, the charge *Q* on the capacitor of the capacitance C_a is

$$Q = C_a V_T e^{i\omega t} = \varepsilon C_o V_T e^{i\omega t} \tag{1.38}$$

where

C_o is the value of the capacitance of the vacuum.

ε is the dielectric permittivity or dielectric constant of the material.

The capacitive current I_C is defined by

$$I_C = \frac{dQ}{dt} = i\omega\varepsilon C_o V_C \tag{1.39}$$

To account for the energy losses a complex dielectric constant is thus; introduced

$$\varepsilon = \varepsilon' - i\varepsilon'' \tag{1.40}$$

where

- ε' is the dielectric constant or true permittivity dielectric constant which described expressed to the stored energy in the material.
- ε'' is the dielectric loss factor or the imaginary permittivity dielectric loss and it described the dissipative energy in the material which is given by (Tareev, 1975)

$$\varepsilon'' = 2\pi\varepsilon_o \frac{\sigma_a}{\upsilon} = \frac{\sigma_a}{\upsilon} 1.8\text{X}10^{10} \tag{1.41}$$

with ε_o is the permittivity of the free space $(10^{-9}/36\pi)F.m^{-1}$ and σ_a is the active volume conductivity. It's magnitude is given by the following relation (Snoek, 1947)

$$\sigma_a = \upsilon \frac{\varepsilon \tan\delta}{1.8\text{X}10^{10}} \Omega^{-1}m^{-1} \tag{1.42}$$

where ν is the frequency of the applied field and $\tan(\delta)$ is the dielectric loss tangent, which is a component of the phase difference between the applied voltage and the total current through the circuit .

The dielectric loss tangent *D* is given by (Tareev, 1975)

$$D = tan\delta = \frac{\varepsilon''}{\varepsilon'} \tag{1.43}$$

The quantity $\tan(\delta)$ sometimes called dissipation factor. As well as the other parameters of the dielectric properties, the value of $\tan(\delta)$ depend on the various external factors such as frequency of the applied voltage.

The behaviour of $\tan(\delta)$ with an applied frequency is represented in figure (1.8). The frequency ω' corresponds to the maximum $\tan(\delta_{\max})$ as illustrated in figure (1.8). (Nwanje, 1980) gives it as

$$\omega' = \sqrt{\frac{1}{\tau^2} + \frac{S_C}{C_g \tau}} \tag{1.44}$$

with

$$\tan(\delta_{\max}) = \frac{S_C \tau}{2C_g \sqrt{1 + (S_C \tau / C_g)}} \tag{1.45}$$

where

C_g is the geometrical capacitance.

S_C is the conduction corresponding to absorption current I_A.

Figure (1.8) becomes especial clear from a physical standpoint in the case of a purely dipole mechanism of losses. The frequency ω' corresponds to such a ratio between the period of an external electric field and the time τ of the relaxation of the dipoles, as it is needed to observe the greatest loss of energy to overcome the resistance of the viscous medium by the dipole. Assuming that $S_C << C_g \tau$, then equation (1.44) becomes

$$\omega' \tau = 1 \tag{1.46}$$

with $\omega' = 2\pi \upsilon_{\max}$ which is defined as the jumping probability per unit time, i.e. hopping probability P, where τ is the relaxation time which is given by the relation ($\tau = 1/2P$ or $\upsilon_{\max.} \propto P$) (Kuanr, Singh, Kishan, Kumar, Rao, Sngh and Sivastava, 1988; Raviner and Kumar, 2001). Equation (1.46) is the condition of the maximum of dielectric losses in the polar dielectric materials.

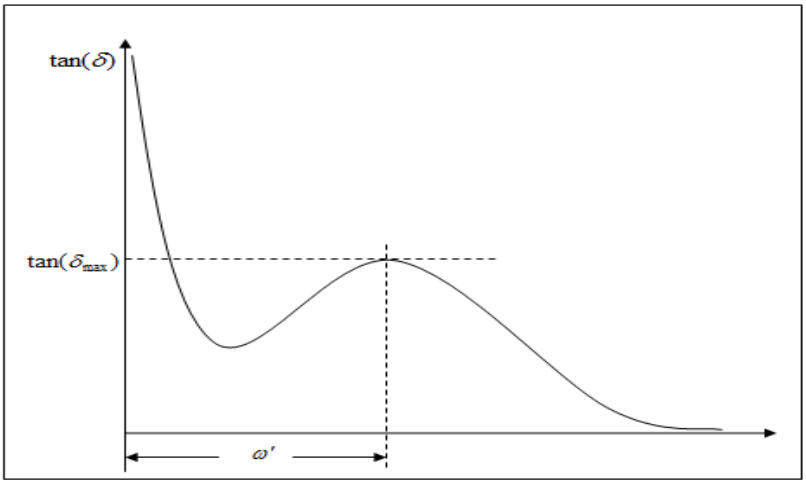

Figure (1.8): Dependence of the loss tangent of the dielectric materials on the applied frequency

CHAPTER 2
Literature Survey

CHAPTER 2

Literature Survey

This chapter contains some of the previous studies for various ferrite systems which have the same trend of the subject of the mixed ***Li-Zn*** spinel ferrite. These studies have illustrated the magnetic, the electric and the dielectric properties for different ferrite systems.

2.1 Magnetic Properties

Sattar et al, (Sattar et al, 2007), studied the effect of Ca substitution on the physical and magnetic properties of $Li_{0.3-0.5x}Zn_{0.4}Ca_xFe_{2.3-0.5x}O_4$ ferrites. They found that the saturation magnetization increases up to x = 0.01 and then it decreases. On the other hand, the initial permeability decreased while the Curie temperature remained almost constant with increasing x.

Maria et al, (Maria, Choudhury and Hakim, 2010), prepared Zn doped Cu ferrite of the composition $Cu_{1-x}Zn_xFe_2O_4$ by standard double sintering ceramic technique. They found that permeability is increase with increase the Zn content up to x= 0.4 and then slightly decreases with further increase in $\boldsymbol{Zn^{2+}}$ ions.

Pissurlekar, (Pissurlekar, 2015), studied the magnetic properties for the mixed ferrite system of $Zn_xNi_{(1-x)}Fe_2O_4$. He reported that, curie temperature decreased as ***Zn*** concentration increased. Saturation magnetization and remnant magnetization, both, continuously increase up to x=0.5, and then decreased for more ***Zn*** content.

2.2 Electric Properties

Dawoud and Shaat, (Dawoud and Shaat 2006), studied the dc conductivity as a function of temperature ranges from 300K to 800K for $Cu_{1-s}Zn_sFe_2O_4$ compounds. Log(σT) against $10^3/T$, this relation illustrates a transition near Curie temperature. Also, they showed that the activation energy in the ferrimagnetic region is found in general to be less than that in paramagnetic region

Krishna et al, (Krishna, Kumar and Ravinder, 2012), studied the electrical conductivity of $Ni_{1-x}Zn_xFe_2O_4$ ferrites. They noticed that the temperature dependence of

the electrical conductivity plot shows a kink, which attributed to ferromagnetic-paramagnetic transition, and they showed that the activation energy obtained from resistivity plots in paramagnetic region is more than that in ferrimagnetic region.

Kumar et al, (Kumar, Sridhar, Ravinder and Krishna, 2014), studied electrical properties of a series of copper substituted nickel nano ferrites with the compositional formula $Ni_{1-X}Cu_XFe_2O_4$. The DC electrical properties were carried out by two-probe method from room temperature to well beyond the Curie temperature. Experimental results that they satisfied, showed that DC electrical resistivity decreases with increase of temperature ensuring the semiconducting nature of the ferrites. The DC electrical conductivity found to increase with increase of Cu content and reaches maximum at x=1.0 at which the activation energy for conduction becomes minimum. The activation energy in the ferrimagnetic region is in general lesser than that in the paramagnetic region. The activation energy was found to decrease with the increase of Cu content. The Curie temperature determined from DC electrical properties was found in satisfactory agreement with that determined from Loria technique. The DC electrical resistivity results are discussed in terms of hopping model.

2.3 Dielectric Properties

Aravind et al, (Aravind, Raghasudha and Ravinder, 2015), prepared nickel substituted lithium nano ferrites with the chemical composition $Li_{0.5-0.5x}Ni_xFe_{2.5-0.5x}O_4$, then measured the dielectric parameters like dielectric constant (ε′), dielectric loss tangent (tanδ) and AC conductivity (σ_{AC}) of the samples using LCR meter at room temperature in the frequency range 20 Hz - 2 MHz.

The value of ε′and tanδ decreases continuously with increasing frequency. After certain frequency, the dielectric parameters become independent of frequency. This fact shows a normal behavior of ferromagnetic materials. They observed that the AC conductivity of the prepared samples shows dispersion with respect to frequency. At lower frequencies, AC conductivity is almost constant. But, after certain frequency it increases rapidly and explained this behavior by Koop's theory.

Krishna et al, (Krishna, Ravinder, Kumar, Joshi, Rana and Lincon, 2012), prepared fine powders of Ni-Zn ferrite with composition $Ni_{1-x}Zn_xFe_2O_4$ and measured Dielectric constant (έ) and loss tangent (tan δ) as a function of frequency. The dielectric constant shows dispersion in the lower frequency region and remains almost constant at higher frequencies. The frequency dependence of dielectric loss tangent (tanδ) is found to be abnormal, giving a peak at certain frequency.

A. Rahman et al, (Rahman, Agami and Eltabey, 2012), studied the frequency, temperature and composition dependence of ac resistivity ρ_{ac}, dielectric constant ε' and dielectric loss tanδ of $Cu_{0.5}Zn_{0.5}Nd_xFe_{2-x}O_4$ ferrites (where x= 0.0, 0.02, 0.04, 0.06, 0.08 and 0.1) at low frequency range. For all samples, ρ_{ac}, ε' and tan δ are found to decrease with increasing the frequency.

CHAPTER 3

Calculations and Experimental Techniques

CHAPTER 3

Calculations and Experimental Techniques

In this chapter the experimental techniques employed for the synthesis of ferrites and some metal oxides belonging to the series $Li_{0.5(1-x)}Zn_xFe_{2.5-0.5x}O_4$ and the method of measuring several properties is presented. It includes a description of the preparation method of the ferrite samples "The Oxide Method". The method of measuring the induction as a function of temperature and the magnetization as a function of a magnetizing field is described. In addition, the apparatus and the electric circuits that used are illustrated throughout this chapter.

3.1 Preparation of Samples

The mixed ***Li-Zn*** spinel ferrite have the chemical formula $Li_{0.5(1-x)}Zn_xFe_{2.5-0.5x}O_4$, it is prepared using the standard double sintering ceramic technique by mixing pure metal oxides according to the following formula:

$$0.25(1-x)Li_2CO_3 + xZnO + (1.25-0.25x)Fe_2O_3 \longrightarrow Li_{0.5(1-x)}Zn_xFe_{2.5-0.5x}O_4 + 0.25(1-x)CO_2$$

High purity oxide materials have been used for the preparation of the investigated polycrystalline ferrites. The weight of each oxide is calculated and listed in table (3.1). The compositions are weighted using a sensitive electric balance with accuracy of 10^{-4} gm. Twenty five grams of metal oxides for each composition of each sample are prepared.

The weighted metal oxides are mixed and then grounded to a very fine powder for 5 hours. The mixed powder of oxides are presintered at 750°C for 3 hours using Muffle Furance. Then the prefired powder was well ground for 3 hours and pressed with hydraulic press under constant pressure of 3×10^8 *pa*, by using a small quantity of butyl alcohol as a binding material. Some samples were pressed in the form of a disc shape which have a radius of 4.95 *mm* and thickness L (4-7) *mm*. Other samples in toroid form with an external radius r_o of 8.2 *mm*, and internal radius r_i of 3.9 *mm* with thickness of (4-5) *mm*. All samples are sintered at 1150^oC for soaking time of 5 hours using Muffle Furance (BIFATHERM model A C62).

After sintering, the samples were cooled down gradually to room temperature. After cooling, the discs samples were polished to obtain the form of circular discs having two uniform parallel surfaces, and it used to measure the *DC* electrical conductivity, the dielectric constant and dielectric loss tangent. The toroidal samples were polished to obtain a uniform shape to measure the magnetization properties and to determine Curie point temperature.

Table (3.1): Weight of each oxide used to prepare the various samples of the mixed ***Li-Zn*** spinel ferrite.

x	The result composition	M. Wt. of Li_2O_3 (gm)	M. Wt. of *ZnO* (gm)	M.Wt.of Fe_2O_3 (gm)
0.0	$Li_{0.5}Fe_{2.5}O_4$	2.1175	0.00	22.8825
0.2	$Li_{0.4}Zn_{0.2}Fe_{2.4}O_4$	1.659	1.8275	21.5135
0.4	$Li_{0.3}Zn_{0.4}Fe_{2.3}O_4$	1.219	3.581	20.2
0.6	$Li_{0.2}Zn_{0.6}Fe_{2.2}O_4$	0.7965	5.2652	18.9382
0.8	$Li_{0.1}Zn_{0.8}Fe_{2.1}O_4$	0.3905	6.8835	17.726
1.0	$ZnFe_2O_4$	0.00	8.44	16.56

3.2 Magnetization Measurements

The measurement of *M* is based on Faraday's law of the electromagnetic induction, using the toroidal sample as shown in figure (3.1). The toroidal samples of the ferrites materials are especially used as a transformer core in the magnetization measurements. Different parameters, that is measured by a micrometer with accuracy 0.01*mm*., can be defined from the figure (3.1) as:

L is the toroidal sample thickness.

r_i is the internal radius of the toroidal sample.

r_o is the external radius of the toroidal sample.

r_m is the average radius of the internal and the external radius of the toroidal sample i.e. $r_m = \frac{r_i + r_o}{2}$

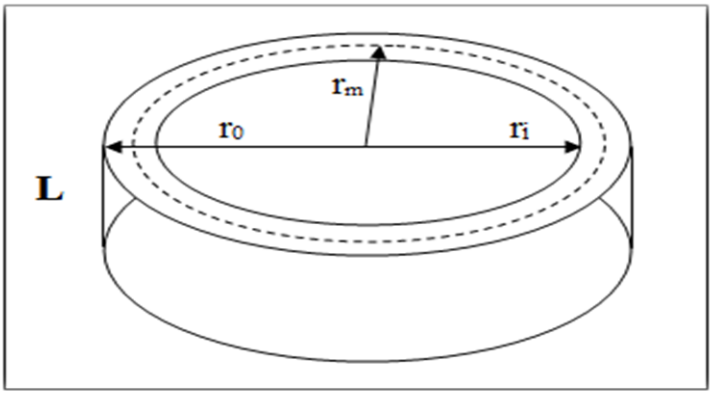

Figure (3.1): A toroidal sample shape.

The $M\ (A.m^{-1})$ is measured at room temperature as a function of the applied magnetizing current which changed in the range from (0 -5A) at constant frequency ν = 50Hz. The corresponding $H\ (A.m^{-1})$ varied in range of (100-1800 $A.m^{-1}$), which is calculated by the equation (3.3). The used circuit in these measurements is shown in figure (3.2).

$M\ (A.m^{-1})$ is calculated from the relation

$$M = \frac{B}{\mu_o} - H \qquad (3.1)$$

The scalar quantity of the flux density B was calculated according to (Jadhav, Devan, Kolekar and Chougule, 2009)

$$B = \frac{50}{\nu}\frac{50}{AN_S}V_S \qquad (3.2)$$

where:

V_s is the induced voltage in the secondary coil,

N_s is the number of turns of secondary coil,

A is the cross sectional area of the toroidal sample [A=L(r_o-r_i)]

(Dawoud, 1997) calculates the $H\ (A.m^{-1})$ from the relation

$$H = \frac{N_P i_P}{2\pi r_m} \tag{3.3}$$

where:

N_p is the number of turns of primary coil

i_p is the current in the primary coil

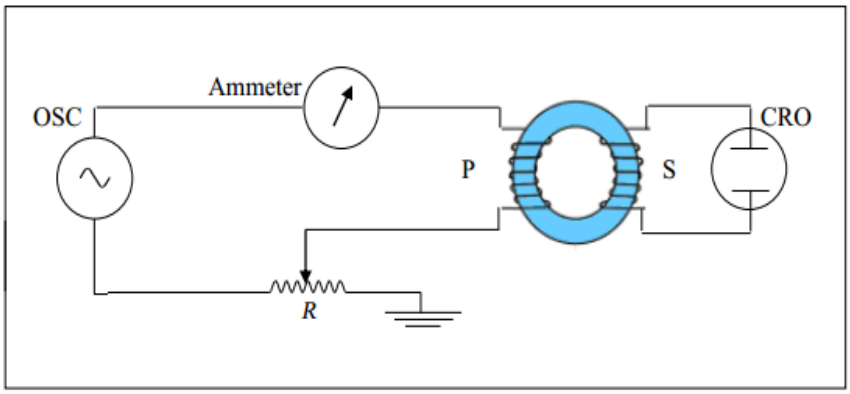

Figure (3.2): Circuit diagram for measuring the magnetization using the toroidal samples of the mixed ***Li-Zn*** spinel ferrite.

3.3 Determination of Curie Point Temperature

In order to determine the Curie point temperature, the inductance *L* of the toroidal sample is measured as a function of temperature. For inductance measurements, LCR meter model (GW- instek LCR-821) is used, with series circuit and applied voltage of 1v and constant frequency of 20 KHz with accuracy of (0.05%).

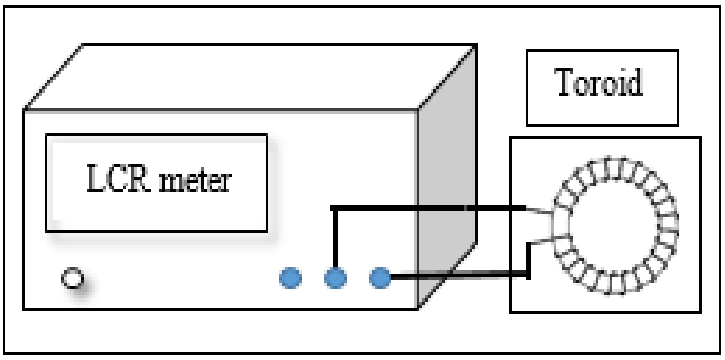

Figure (3.3): Circuit diagram for measuring the inductance of the toroidal samples of the mixed ***Li-Zn*** spinel ferrite.

3.4 Measurements of DC Electrical Conductivity

DC electrical conductivity ($\sigma_{DC}\,\Omega^{-1}m^{-1}$) is one of the useful characterization techniques to understand conductivity mechanism. The σ_{DC} of the samples is estimated at different temperature by two-probe method. That is, pellets of a disk-shape are smoothed to have uniform plane surface. Silver is pasted on both sides to ensure good electrical contacts and two silver wires, with high purity, are used as electrodes.

A digital multimeter (model FLUKE -177) was used to measure the resistance of the samples. The σ_{DC} of the samples are calculated from the formula :

$$\sigma_{DC} = R^{-1}\frac{L}{A} \tag{3.4}$$

where:-

R : Resistance of the sample

L : Length of the sample which was measured by a micrometer of accuracy 0.01 *mm*

A : Cross – sectional area of the sample .

The σ_{DC} is measured in wide range of temperature, from room temperature up to beyond Curie temperature with three-degrees step. The increasing of temperature is carried out gradually. The temperature dependence of the σ_{DC} plot is expected to show a kink, which can be attributed to ferrimagnetic-paramagnetic transition.

3.5 Characterization of the AC Conductivity and Dielectric Properties

An AC field was established across the samples in order to measure the AC conductivity($(\sigma_{AC})\Omega^{-1}.m^{-1}$), dielectric constant ($\varepsilon$) and dielectric loss tangent ($\tan\delta$) over a variable range frequency in range of 10^4 to 10^6 *Hz* at room temperature, as indicated in Figure (3.4) which consists of:

1- Function signal generator power amplifier (OSC)(model MFG-8250A) was connected across the sample S and standard non inductive resistance R, where the value of R depends upon the resistance of the each sample.

2- Adual-channel oscilloscope (CRO) (GW modelGOS-620) used to measure:

i- The total input voltage V_T connect on X- channel .

ii- The potential V_R drop across the standard non inductive resistance connect on Y- channel .

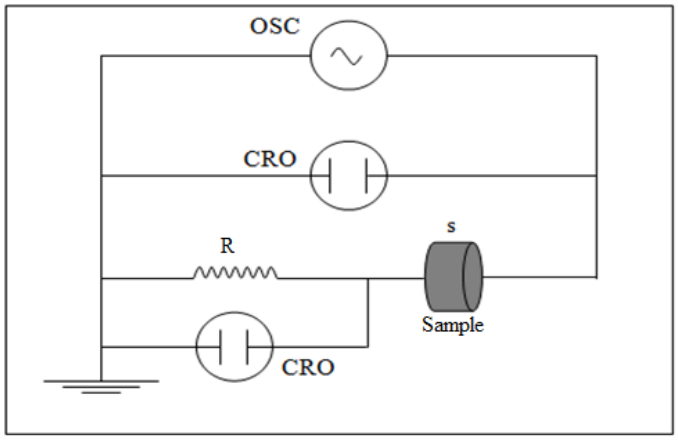

Figure (3.4): Circuit diagram for measuring the dielectric loss tangent using the disc samples of the mixed ***Li-Zn*** spinel ferrite.

Since the sample and resistance R in series, then the AC current passing through the sample can be calculated from Ohm's Law ($I_T = V_R / R$) and σ_{AC} can be calculated from:

$$\sigma_{AC} = Z^{-1} \frac{L}{A} \tag{3.5}$$

Where Z is the impedance of the sample, which is calculated by $Z = V_T / I_T$.

According to (Collectt and Katsubel, 1973) the values of $\tan\delta$ were obtained from Lissajous figure displayed on along cathode ray oscilloscope. Referring to figure (3.4), let V_T be the voltage applied to X- plates and V_R to Y plates .

If $$V_X = V_T \sin(\omega t) \tag{3.6}$$

Then $$V_Y = V_R \sin(\omega t + \varphi) \tag{3.7}$$

where φ is the phase angle. These two signals form a Lissajous figure as shown in the figure (3.5). Referring to this figure, when $V_Y = 0$, then $V_X = V_\theta$

If $V_Y = 0$, this implies that $(\omega t + \phi) = \pi$ or $\omega t = \pi - \phi$. Therefore, we find that

$$V_\theta = V_T \sin(\pi - \varphi) = V_T \sin(\varphi) \tag{3.8}$$

Hence, the dielectric loss tangent $\tan\delta$ is given by the following:

$$\tan\delta = \cot\varphi \tag{3.9}$$

$$\tan\delta = \frac{\sqrt{(V_T^2 - V_\theta^2)}}{V_\theta} \tag{3.10}$$

where V_T and V_θ can be readily measured on the cathode ray oscilloscope, then the value of $\tan\delta$ can be computed from the equation (3.10) (Dugdal, 1977).

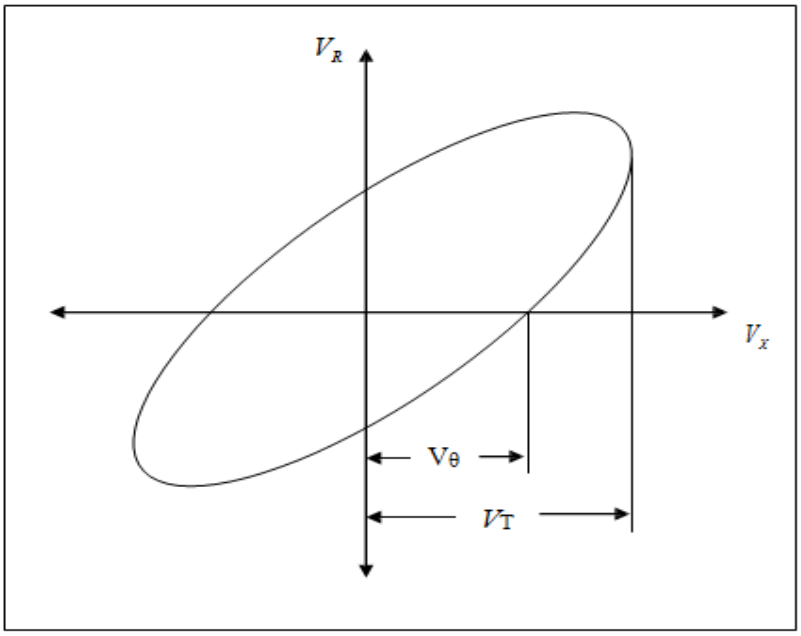

Figure (3.5): Lissajous figure of the input voltage V_T and the current passing through the sample.

CHAPTER 4

Results and Discussion

CHAPTER 4

Results and Discussion

The experimental results of some magnetic, electric and dielectric quantities for the mixed ***Li-Zn*** spinel ferrite in the form of, $Li_{0.5(1-x)}Zn_xFe_{2.5-0.5x}O_4$, are recorded and briefly discussed in this chapter.

4.1 Magnetic Properties

The magnetic properties of the mixed ***Li-Zn*** spinel ferrite depend on the percentage of Zn^{2+} composition. The variation of magnetic properties of $Li_{0.5(1-x)}Zn_xFe_{2.5-0.5x}O_4$ can be understood in term of cations distribution and exchange interactions between the two sub lattices of spinel structure, T_d and O_h sites.

4.1.1 Magnetic Moment

The net magnetization (*M*) is defined as the net magnetic moment (μ_{net}) per unit volume for each sample in Bohr magnetos unit (μ_B). The μ_{net} is calculated according to the expected cations distribution for the mixed ***Li-Zn*** spinel ferrite, in which T_d site is occupied by Zn^{2+} and Fe^{3+} ions, and the O_h site is occupied by Li^{1+} and Fe^{3+} as following

$$(Zn_x^{2+}\ Fe_{(1-x)}^{3+})\ \{Li_{0.5(1-x)}^{1+}\ Fe_{1.5+0.5x}^{3+}\}\ O_4^{2-} \qquad (*)$$

The Zn^{2+} ions show a marked stronger preference for the T_d site than the Fe^{3+} ions, depending upon their electronic configuration (Vishwanathan and Murthy, 1990), where their (4s 3d) electrons form a covalent bonds with 2p electrons of the oxygen ion (Belled, Pujar and Chougule, 1998; Tang, Manthiram and Goodenough,1989).

The μ_{net} in the spinel structure is defined as the difference between the magnetic moments of T_d and O_h sites, μ_T and μ_O respectively. Where μ_T is the magnetic moment for T_d and μ_O is the magnetic moment for O_h. The values of μ_T, μ_O and μ_{net}

are calculated according to the cations distribution which is given in (*) (Dawoud, 1997; Tayal, 1998)

$$\mu_T = 2(1\text{-}x)\ S_m\ \mu_B \quad (4.1)$$

$$\mu_O = 2(1.5\text{+}0.5x)\ S_m\ \mu_B \quad (4.2)$$

$$\left|\vec{\mu}_{net}\right| = \left|\vec{\mu}_o\right| - \left|\vec{\mu}_T\right| \quad (4.3)$$

where $S_m = 5/2$ is the spin quantum number of the $\boldsymbol{Fe^{3+}}$ ions, but $\boldsymbol{Zn^{2+}}$ ions and $\boldsymbol{Li^{1+}}$ ions have zero spin quantum number. The calculated values of μ_O, μ_T and μ_{net} are listed in table (4.1) and their variation with the composition x are represented in figure (4.1).

Table (4.1): Calculated values of μ_O, μ_T and μ_{net} according to the cations distribution of the mixed ***Li-Zn*** spinel ferrite.

x	$(\mu_O)\mu_B$	$(\mu_T)\mu_B$	$(\mu_{net})\mu_B$
0.0	7.5	5	2.5
0.2	8	4	4
0.4	8.5	3	5.5
0.6	9	2	7
0.8	9.5	1	8.5
1.0	10	0	10

Previous studies (Chinnassamy, Narayanaasmy, Poupandian and Chattopadhyay, 2001; Jacob, Thankachan and Xavier, 2013; Upadhyay, Verma, Rath, Sahu, Anand, Das and Mishra, 2001) are reported that, the mixed ***Li-Zn*** spinel ferrite in the bulk form gives a normal spinel ferrite with the $\boldsymbol{Zn^{2+}}$ ions at the T_d site, while the $\boldsymbol{Fe^{3+}}$ ions at the O_h site. When the $\boldsymbol{Zn^{2+}}$ ions increase the cations distribution is not altered, but the exchange interaction between T_d and O_h sublattices getting weakened. However, the exchange interaction between T_d and O_h sublattices go through a change in its tendency from ferrimagnetic state to antiferromagnetic state (Crangle, 1991; Kumar, Sridhar et al,

2014). The μ_{net} in the mixed ***Li-Zn*** spinel ferrite structure is enhanced with increasing Zn^{2+} concentration, for the sample $ZnFe_2O_4$ at x =1.0, which represents a high concentration of Zn^{2+}, the Zn^{2+} ions weakens the super-exchange interaction between the magnetic ions, so $ZnFe_2O_4$ represents an antiferromagnatic characteristic.

It is clear from figure (4.1) that, the magnitude of μ_T decreases with increasing of Zn^{2+} ions, but the magnitude of μ_O and the μ_{net} increase with increasing of Zn^{2+} content. The variation of the μ_{net}, μ_O and μ_{net} with the Zn^{2+} content can be explained by assuming that, the increment of the non-magnetic Zn^{2+} ions substituted ions in the T_d implies to transfer Fe^{3+} ions from T_d site to the O_h site, this will increase the concentration of Fe^{3+} ions in O_h site. This tends to increase μ_O and decrease μ_T. Therefore, μ_{net} would rise linearly with the Zn^{2+} ions and would reach value $10\mu_B$ per molecule might be expected on x =1.0, when all Fe^{3+} ions have been replaced by the Zn^{2+} ions.

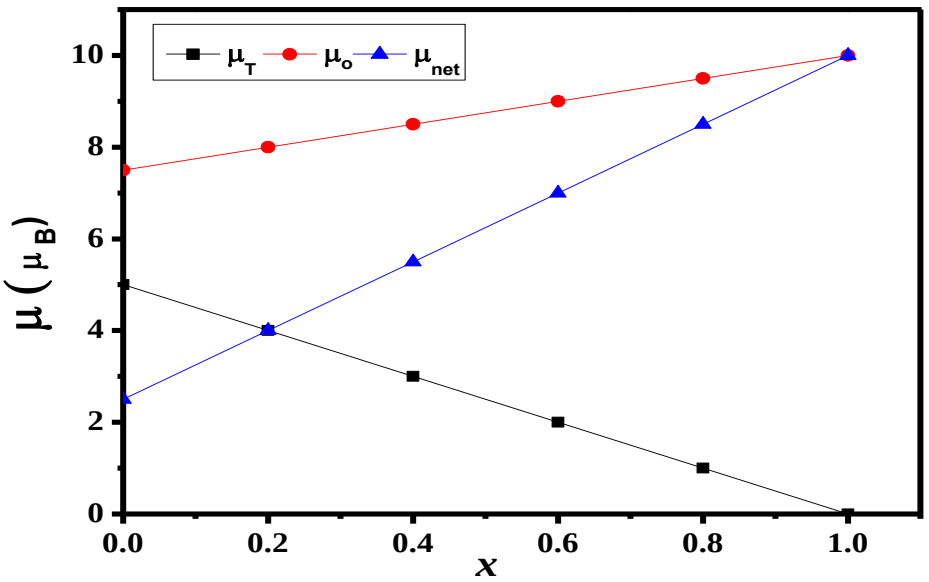

Figure (4.1): Variation of μ_O, μ_T and μ_{net} with the Zn^{2+} ratio.

4.1.2 Ionic radii for Tetrahedral and Octahedral Sites

The ionic radii for the T_d and the O_h sites, are calculated using equations (Potakova, Zverv and Romanov, 1972; Standly, 1972)

$$R_T = x\,R_{Zn^{2+}} + (1\text{-}x)\,R_{Fe^{3+}} \quad (4.4)$$

$$R_O = \frac{1}{2}[\,0.5(1\text{-}x)\;R_{Li^{1+}} + (1.5+0.5x)\;R_{Fe^{3+}}\,] \quad (4.5)$$

where R_T and R_O are the mean ionic radii per molecule for the T_d and the O_h sites, respectively. $R_{Zn^{2+}}$, $R_{Fe^{3+}}$ and $R_{Li^{1+}}$ (0.68 nm) are the ionic radii of the Zn^{2+} ion (0.68 nm) (Lodders and Fegly, 1998) , Fe^{3+} ion (0.64 nm) and Li^{1+} ion (0.68 nm) respectively (Dawoud, 1997).

The calculated values of R_T , R_O and R_T/R_O for the mixed ***Li-Zn*** spinel ferrite are listed in table (4.2). The ionic radii R_T and R_O are plotted versus the Zn^{2+} content in figure (4.2), while R_T/R_O versus the Zn^{2+} content is plotted in figure (4.3). From these figures, it is noticed that, R_T increases while R_O decreases with increasing of the Zn^{2+} ions. The increasing of R_T is attributed to the replacement of the Fe^{3+} ions by the larger ionic radius of the Zn^{2+} ions in the T_d site. The increment of Fe^{3+} ions, which has smaller radius than Li^{1+} ions, in O_h site tends to decrease R_O .

Table (4.2): Calculated values of R_T , R_O and R_T/R_O for the mixed ***Li-Zn*** spinel ferrite.

x	R_T (nm)	R_O (nm)	R_T / R_O
0.0	0.064	0.065	0.984615
0.2	0.0648	0.0648	1.0
0.4	0.0656	0.0646	1.01548
0.6	0.0664	0.0644	1.031056
0.8	0.0672	0.0642	1.046728
1.0	0.068	0.064	1.0625

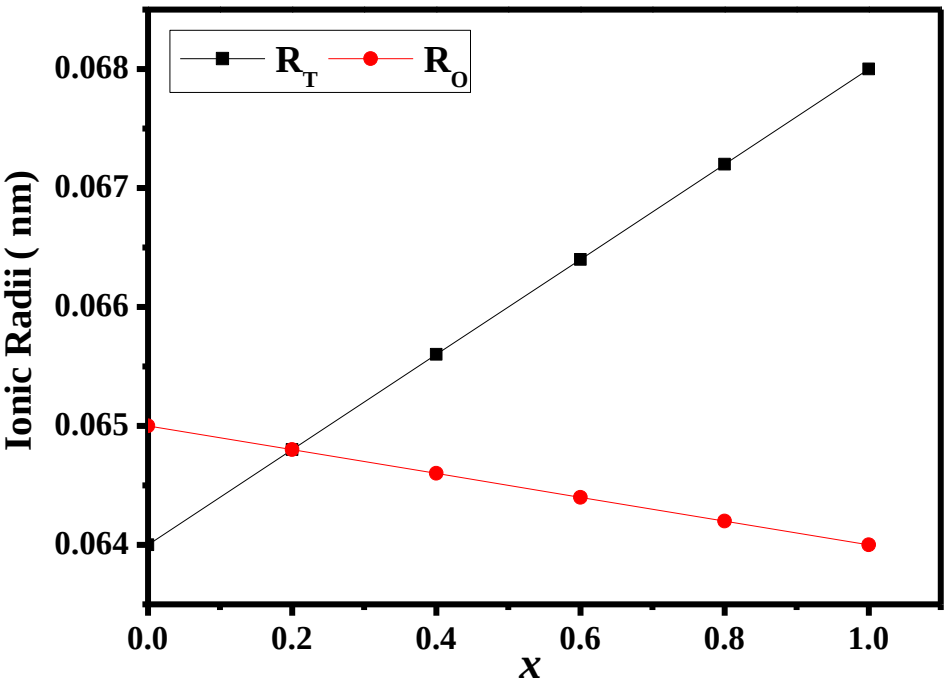

Figure (4.2): Variation of R_T and R_O with the Zn^{2+} ratio.

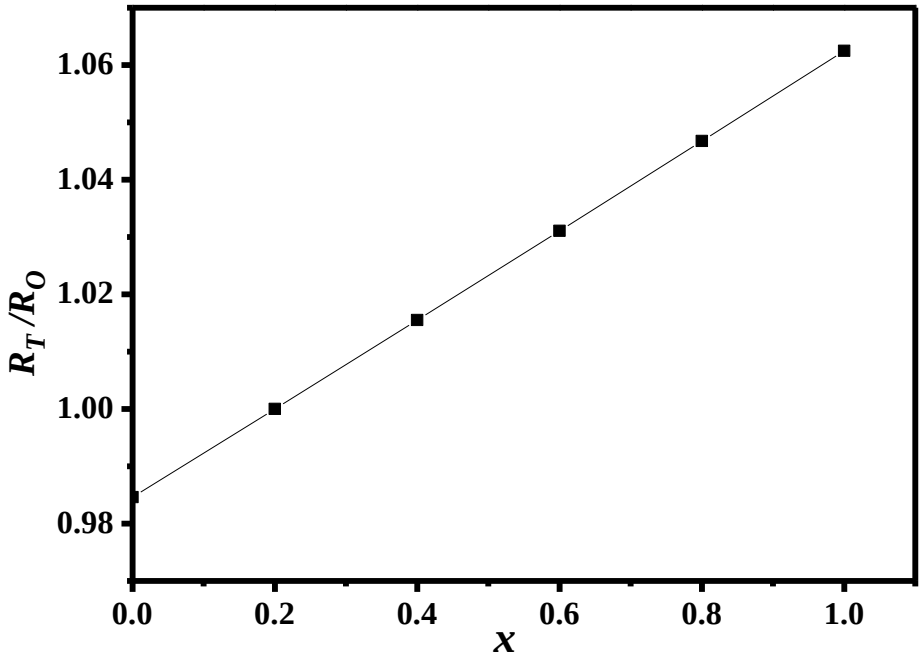

Figure (4.3): Variation of R_T/R_O with the Zn^{2+} ratio.

4.1.3 Magnetization Study

The relation between the net magnetization M ($A.m^{-1}$) and the applied magnetic field intensity H ($A.m^{-1}$), in the range of (148-1856) $A.m^{-1}$, for the ferrite samples of the system $Li_{0.5(1-x)}Zn_xFe_{2.5-0.5x}O_4$ are studied at room temperature. The obtained results for all the ferrite samples are illustrated in figure (4.4), where the variation of M and H for the samples with different composition are plotted.

The calculated M of the samples does not exhibit a saturation magnetization. The saturation magnetization of a mixed ***Li-Zn*** spinel ferrite at the absolute zero point would be expected to increase with increasing of the Zn^{2+} ions. Thus, the remarkable fact appears that, the substitution of magnetic ions in a ferrimagnetic materials by the non-magnetic such Zn^{2+} and Cd^{2+} ions lead to an increase in the saturation magnetization (Verwey and Helimann, 1947).

Figure (4.5) shows that for mixed ***Li-Zn*** spinel ferrite samples with $x \leq 0.6$ the M increase with increasing of the Zn^{2+} ions. This increase may be attributed to the fact that, small amount of Zn^{2+} ions occupy T_d site displacing Fe^{3+} ions from T_d site to O_h site and increasing the content of Fe^{3+} ions in O_h site. That is the low Zn^{2+} concentration reduces the number of spins occupying T_d site, causing M to increase (Sattar, Wafik, El-Shokrofy and El-Tabby, 1999). The obtained results agreed well with the results obtained earlier (Dawoud and Shaat, 2006; Pissurlekar, 2015; Sattar et al, 2007).

Figure (4.6) shows the variation of M for different values of H. At H=148 $A.m^{-1}$, M is increased with increasing of Zn^{2+}ions. For H=1188 $A.m^{-1}$, M is increased to x = 0.2, then M does not change for $x \geq 0.2$, but for H=1856 $A.m^{-1}$, M is increased up to x = 0.2 then it decrease after that. The behavior of M for H=1188 and 1856 $A.m^{-1}$ may be related to the demagnetization factor for the samples with $x \geq 0.2$, i.e. with increasing of Zn^{2+} ions in the mixed ***Li-Zn*** spinel ferrite.

The increase of M with increasing $\boldsymbol{Zn^{2+}}$ ions can be explained by Neel's two-sublattice model of the magnetic theory of the ferrimagnetic materials. In this model Néel considered that ferrimagnetic crystal lattice could be divided into two magnetic sublattices or groups, i.e. T_d and O_h sites, in the spinel lattice structure, where μ_T and μ_O are not equal, so that, μ_{net} can be found. This happens either because they are made from elements in different ionic state, e.g. $\boldsymbol{Fe^{2+}}$ and $\boldsymbol{Fe^{3+}}$, or from different elements in the same or different ionic states, e.g. $\boldsymbol{Cu^{2+}}$ and $\boldsymbol{Fe^{3+}}$ (Dawoud and Shaat 2006). Owing to the presence of the non-magnetic $\boldsymbol{Zn^{2+}}$ ions at the T_d site, the magnetization of the T_d lattice will be smaller than the magnetization in the normal ferrite, since, the $\boldsymbol{Fe^{3+}}$ ions have the largest magnetic moment are positioned at the O_h site.

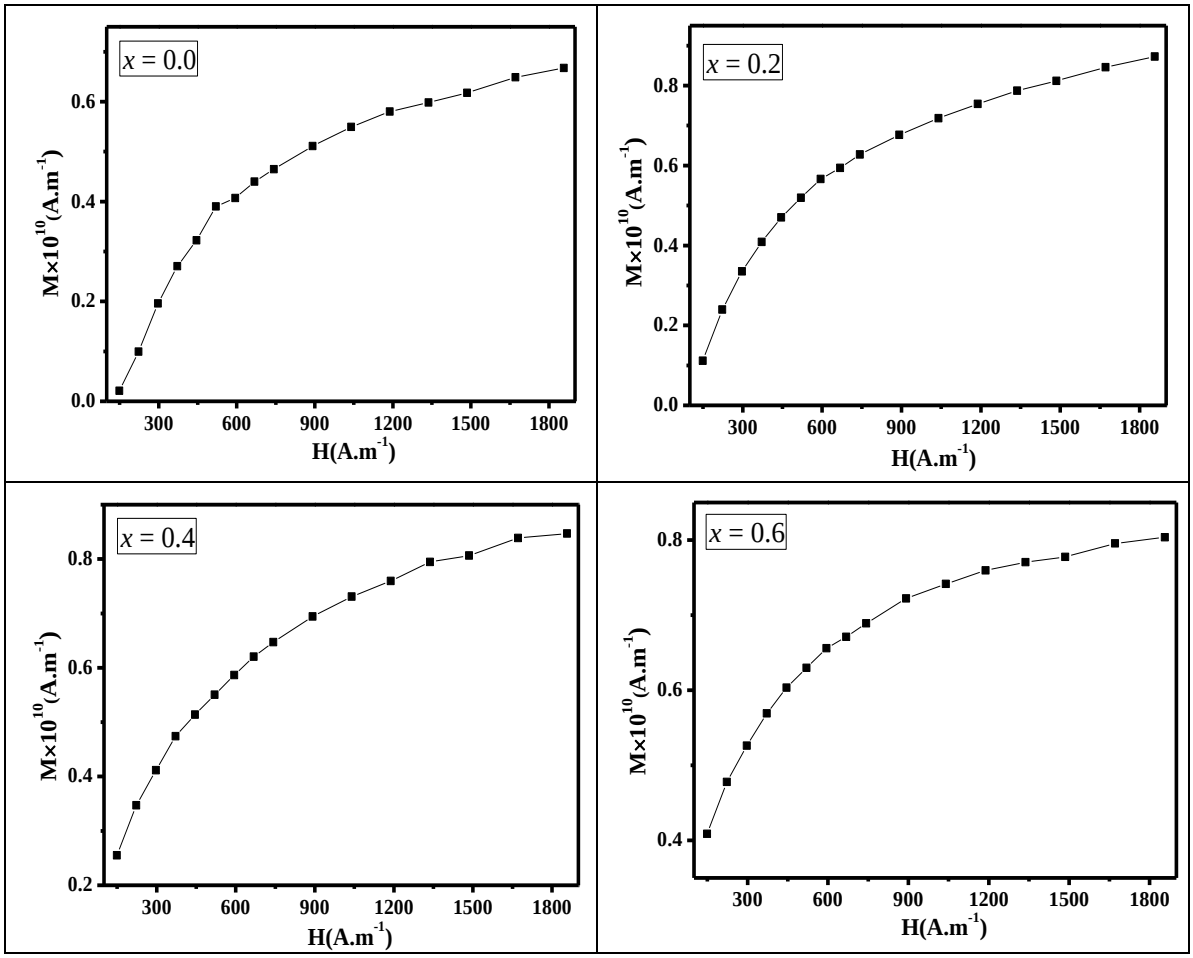

Figure (4.4): Variation of M with H for the samples with x = 0.0, 0.2, 0.4, and 0.6.

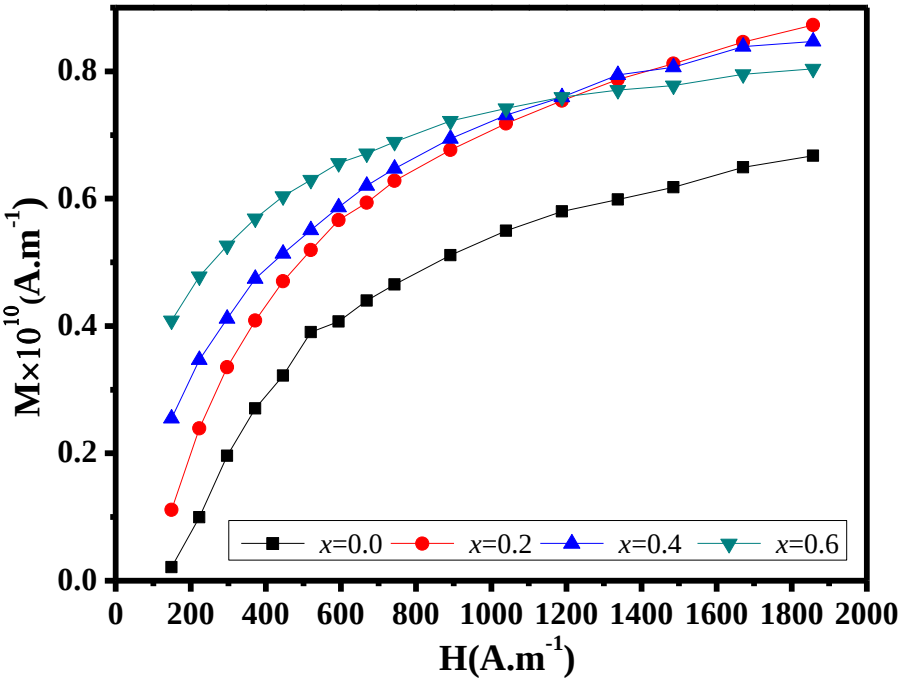

Figure (4.5): Variation of M with H for all the samples for different compositions.

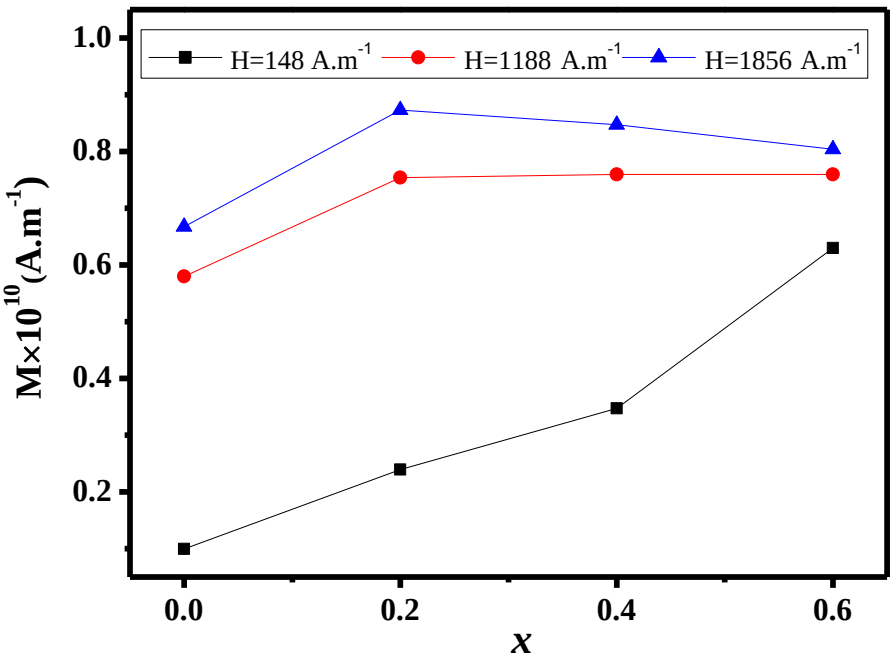

Figure (4.6) : Variation of M with the composition x for different values of H .

4.1.4 Relative Permeability

The relative permeability (μ_r) for all samples gives the description of the magnetization behavior during the change of the exposed external applied field. It is defined as the ratio between the induction field (*B)* and *H*, in the form $\mu_r = B/\mu_o H$, the relation between *H* and μ_r has an interesting behavior for the present ferrite samples as shown in figure (4.7).

The behavior of μ_r versus *H* for samples of *x=0.0* and *x=0.2*, was divided into two stages a and b as in figure (4.7). In stage a, μ_r increases with increasing of *H* up to *H* =300 $A.m^{-1}$ then μ_r decreases. The increasing of *H* causes a very rapid increase in *B*, which imply to increase μ_r . This behavior can be related to the aligning effect of *H* on the ionic spins. In stage B, μ_r decreasing with increasing of *H* might be cause a slight increase of *B*, which can be explained as that two samples have the highest spin ordering. This means that, the ionic ordering of these two samples is closer to the saturation state. The same behavior was observed by H. Dawod (Dawod, 1997).

For the samples of *x=0.4* and *x=0.6*, μ_r decreases exponentially with increasing of *H*. As shown in figure (4-7). The decreasing of μ_r for these two samples may attributed to the lowest ordering spin of them.

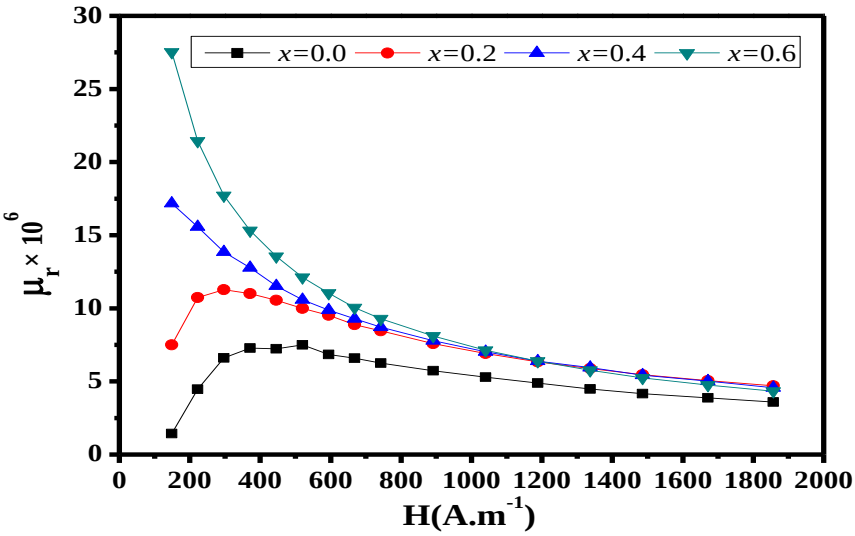

Figure (4.7): Variation of μ_r with *H* for the samples with composition *x* =0.0, 0.2, 0.4 and 0.6.

4.2 Electric Properties

4.2.1 Induction and Curie Temperature Point

The interested way to determine Curie temperature point (T_C) of a ferrite is to measure the inductance, *L(T)*, of a coil wrapped on a ferrite core, preferably of toroidal shape, as a function of temperature.

The permeability (μ) of the ferrimagnetic materials which results from the domains walls motion and spin rotational (Shaat, 2012). It depends upon the magnetaization, the ionic structure and the degree of domain walls continuity across the grain boundary layers (Dawoud and Shaat, 2006). It is found that μ varies with different conditions such as the soaking time, the sintering temperature, the time of sintering, the porosity, the defects introduced and atmosphere of firing due to the sintering process (Shaat, 2012).

The relation between *L* of a closed packed coil (toroid) knitted around a substance and it is permeability is given by (Akhtar, Yahya and Hussain, 2009; Jebeli and Mohamed, 2013)

$$\mu = \frac{2\pi L}{N^2 l \ln\left(\frac{r_o}{ri}\right)} \tag{4.6}$$

where *N* is the number of turns, r_i and r_o are inner and outer radii of toroid, respectively, and *l* is thickness of torroid. The permeability of the substance can be expressed by

$$\mu = \mu_o \mu_r \tag{4.7}$$

where μ_o is the free space permeability and μ_r is the relative permeability. However, μ_r at low excitation level and constitutes the most important means for the comarison of soft magnetic materials can be defined as the initial permeability (μ_i). Therefore, an expression for the initial permeability can be derived as follows

$$\mu = \frac{2\pi L}{\mu_o N^2 l \ln\left(\frac{r_o}{ri}\right)} \tag{4.8}$$

The M of a specific core material located inside the coil has the following expression (Shaat, 2012; Nabiyouni, Fesharaki, Mozafari and Amighian, 2010)

$$M = \chi_m H = \frac{(\mu_i - 1)}{4\pi} H \tag{4.9}$$

where χ_m is the magnetic susceptibility. Using equations (4.8) and (4.9), it can be found that

$$M = \left[\frac{L}{\mu_o N^2 l \ln\left(\frac{r_o}{r_i}\right)} - \frac{1}{4\pi} \right] H \tag{4.10}$$

It is clear from equation (4.10) that, M is proportional to L. This means that, if L changes with temperature, M also changes. Therefore, the transition or Curie temperature can be indicated from the variation of L with temperature.

The variation of L for the toridial shape samples of mixed ***Li-Zn*** spinel ferrites have been investigated from room temperture to fit beyoud the T_C . Figure (4.8) gives a plot of L versus temperature, it can be seen that, for samples of $x \leq 0.6$, the value of L increases with increasing of temperture up to a certain temperture T_C . At this point a sharp drop of L is occurred, proving that at this point the sample is changed from ferrimagnetic to paramagnetic. It is found that samples of $x \geq 0.8$ have no transition, which implies that they are paramagnatic at room temperture. Values of T_C are detrmined along with the value of x in table (4.3). And also T_C values for different samples with composition x are depicted in figure (4.9). From this figure, it is seen that T_C decreases with increasing of $\boldsymbol{Zn^{2+}}$ ions up to x = 0.6. This is attributed to the decrease of $T_d - O_h$ interaction. As the content of $\boldsymbol{Zn^{2+}}$ ions is increased, the relative number of $\boldsymbol{Fe^{3+}}$ ions at T_d site decreases, which causes a reduction in the $T_d - O_h$ interaction (Shinde, Gadkari and Vasambekar, 2013). The decrease in the T_C with increasing of $\boldsymbol{Zn^{2+}}$ ions in the different ferrimagnetic materials was, also, observed by other researchers (Alone and Jadhav, 2008; Pissurlekar, 2015).

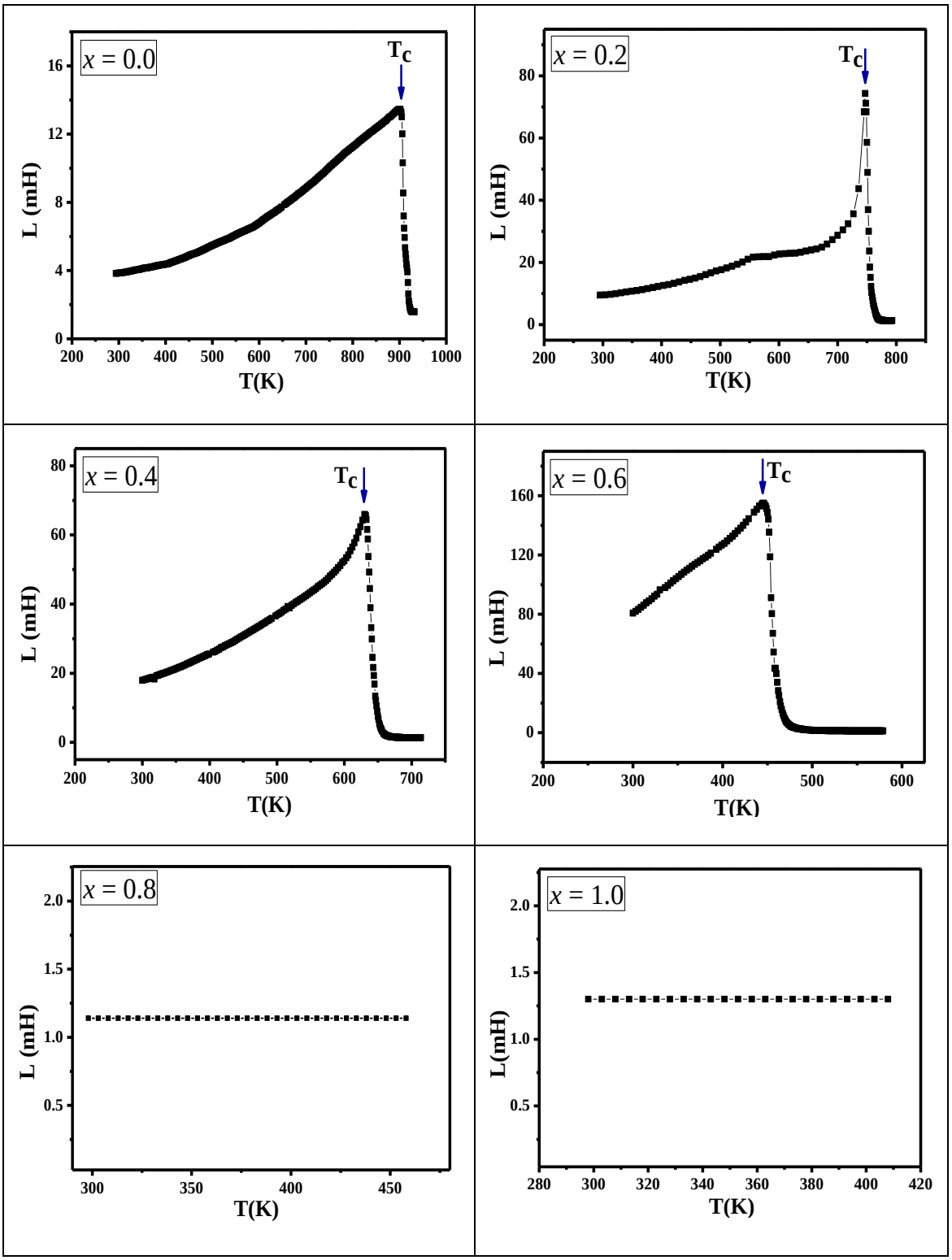

Variation of *L* with temperature for differnet composition *x* = 0.0, 0.2, 0.4, 0.6, 0.8 and 1.0

Table (4.3): Values of T_C that is determined by the induction measurements and the DC conductivity measurements for the mixed ***Li-Zn*** spinel ferrite.

x	Induction Results	DC conductivity Results
	$(T_C)K$	$(T_C)K$
0.0	900	843
0.2	769	728
0.4	628	583
0.6	448	488
0.8	-	-
1.0	-	-

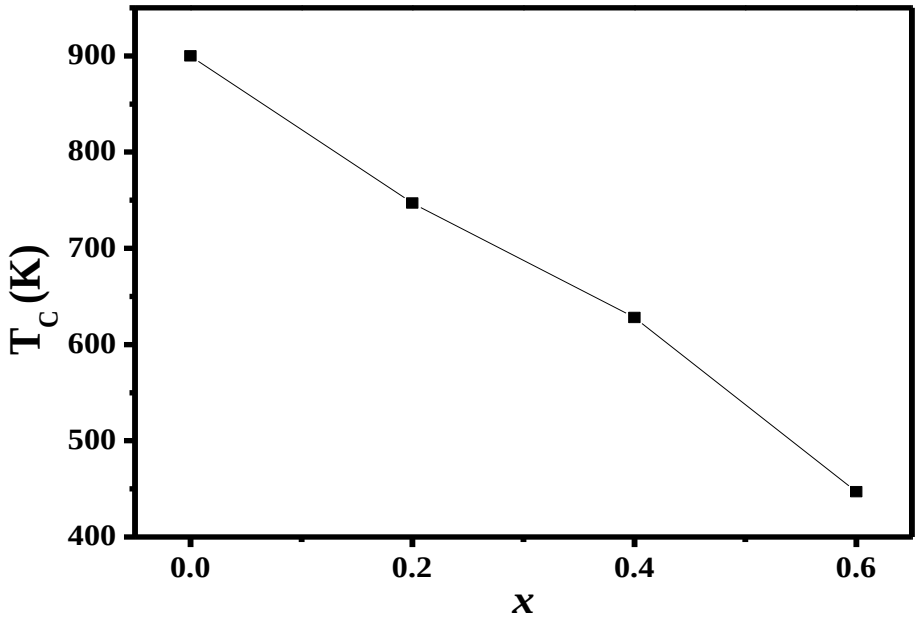

Figure (4.9): Variation of T_C with Zn^{2+} ratio .

4.2.2 Temperature-Dependence of DC Conductivity

In order to understand the temperature dependence of electrical conductivity (σ) of mixed ***Li-Zn*** spinel ferrite of different compositions, electrical conductivity has been investigated from room temperature to fit beyond T_C for each sample.

The experimental dependence of $\ln\sigma$ with the reciprocal of temperature ($10^3/T$) is depicted in figure (4.10). From this figure, it is seen that, $\ln\sigma$ continuously increases with increasing of the temperature that emphasized the semiconductor nature of synthesized samples. This behaviour was found in various ferrite systems (Alone and Jadhav, 2008; Dawoud and Shaat, 2006).

The dependence of σ on temperature in the figure (4.10) fulfils the relation (Blechstein, 1938)

$$\sigma = \frac{S'''}{T} e^{(-E_a/kT)} \tag{4.11}$$

Here S'' is a constant given by ($ne^2d^2\nu/k$) (Heikes and Johnston, 1975), where:

d: is the distance between the nearest neighbor cations

ν : is the frequency of the vibration of the crystal lattice

n: is the number of the charge carriers.

k: is Boltzmann constant

e: is electron charge

Figure (4.11) gives a plot of $\ln\sigma T$ versus ($10^3/T$). It can be seen that, for samples with $x \leq 0.6$ the value of $\ln\sigma T$ increases linearly with temperature up to a certain temperature at this temperature a change of slope has occurred. This change of slope is attributed to change in conductivity mechanism (Kumar et al, 2014). And the sample changing from ferrimagnetism to paramagnetism.

However, this change of slope cannot be observed in compositions with $x \geq 0.8$, that they are considered paramagnetic materials at room temperature. Similar behavior of

these compositions is already observed from the induction study (sec. 4.2.1). Also this behavior was shown in the ***Cd*** spinel ferrite, which is found as diamagnetic substance at room temperature (Ravinder, 2000).

Values of T_C that is determined by induction measurement and DC conductivity measurement for the mixed ***Li-Zn*** spinel ferrite are listed in table (4.3) (see p.55). It is notice that the transition temperature in DC experiment is around the values of T_C from induction experiment indicating that the change in the slope in each case has occurred around T_C point of the corresponding ferrite sample. From the same table it is noticed that, there is a small deviation of the T_C value in the induction measurements than the DC conductivity measurements. This indicates that, the magnetic transition can be manifested in the transport property.

The activation energy values of before and after Curie point transition are calculated from figure (4.11) and are presented in table (4.4). This table includes the value of the activation energies in Ferrimagnetic region (E_f), before Curie point, and paramagnetic region (E_p), after Curie point, for the studied compositions at certain temperature. It is noticed that, E_f vary from 0.51 *eV* to 0.29 *eV* for the samples with $x \leq 0.6$ and E_p vary from 0.62 *eV* to 0.42 *eV*. While the activation energies cannot be determined for the samples with $x \geq 0.8$ since they are paramagnetic at room temperature.

It is clear from (ΔE) that, the values of E_f are smaller than E_p, this is also was found by (Dawoud and Shaat, 2006; Raut, Khirade, Humbe, Jadhav and Shengule, 2016). The decrease in activation energy may be due to the decrease in resistivity with increasing Zn^{2+} concentration because activation energy behaves in the same way as resistivity (Alone and Jadhav, 2008; Mazen, 2000). Generally, the change of slope is attributed to change in conduction mechanism. The conduction at a lower temperature (below T_C) is due to hopping of electrons between Fe^{2+} and Fe^{3+} ions, whereas at a higher temperature (above T_C) is due to hopping of polarons (Klinger, 1977; Kumar and Ravinder, 2001) .

Table (4.4): Values of the activation energies E_f and E_p for the mixed ***Li-Zn*** spinel ferrite.

x	Activation Energy		
	$(E_f)eV$	$(E_p)eV$	$(\Delta E)eV$
0.0	0.51	0.62	0.11
0.2	0.37	0.49	0.12
0.4	0.34	0.44	0.10
0.6	0.29	0.42	0.13
0.8	-	-	-
1.0	-	-	-

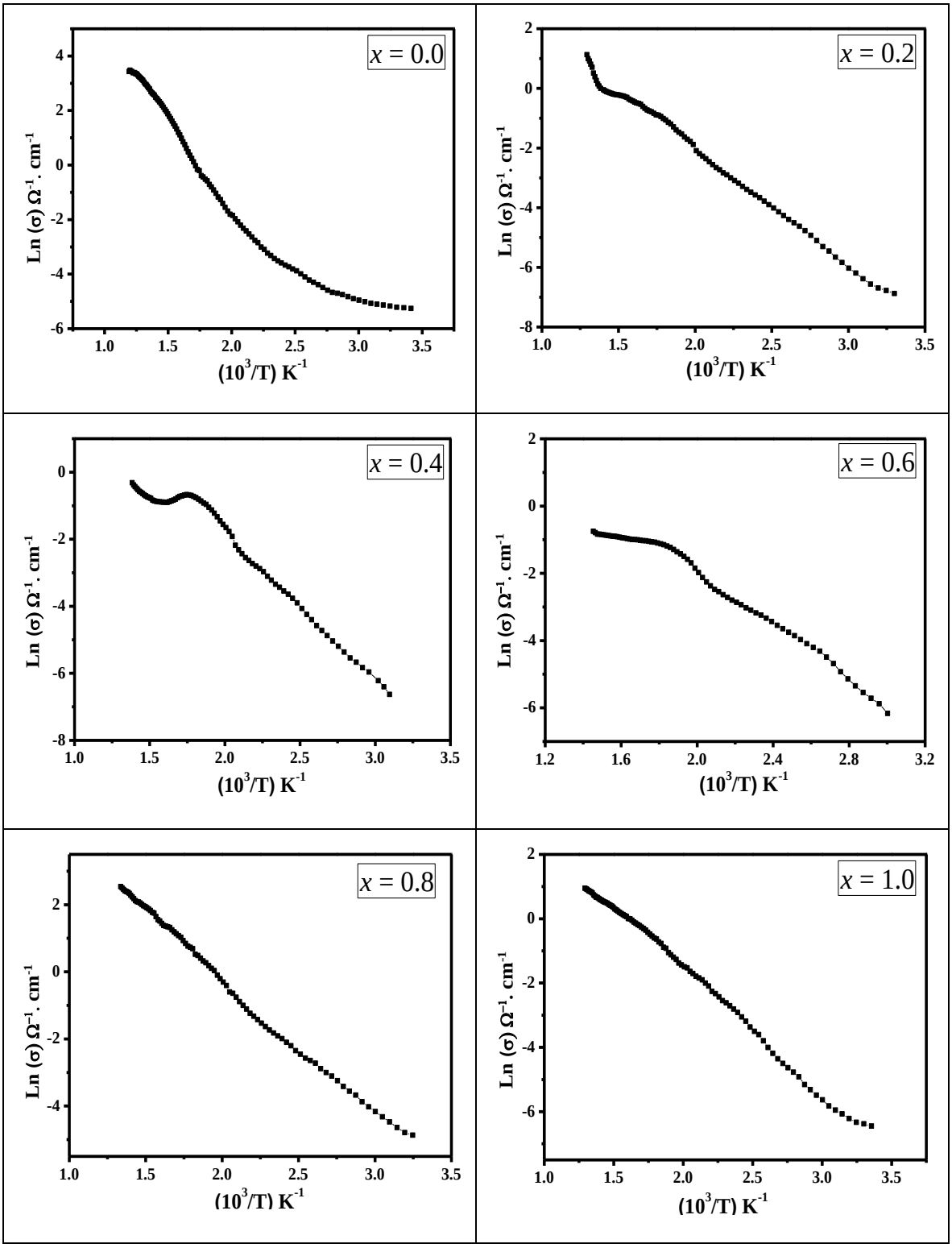

Figure (4.10): Variation of $\ln \sigma$ with ($10^3/T$) For the samples with x=0.0, 0.2, 0.4, 0.6, 0.8 and 1.0

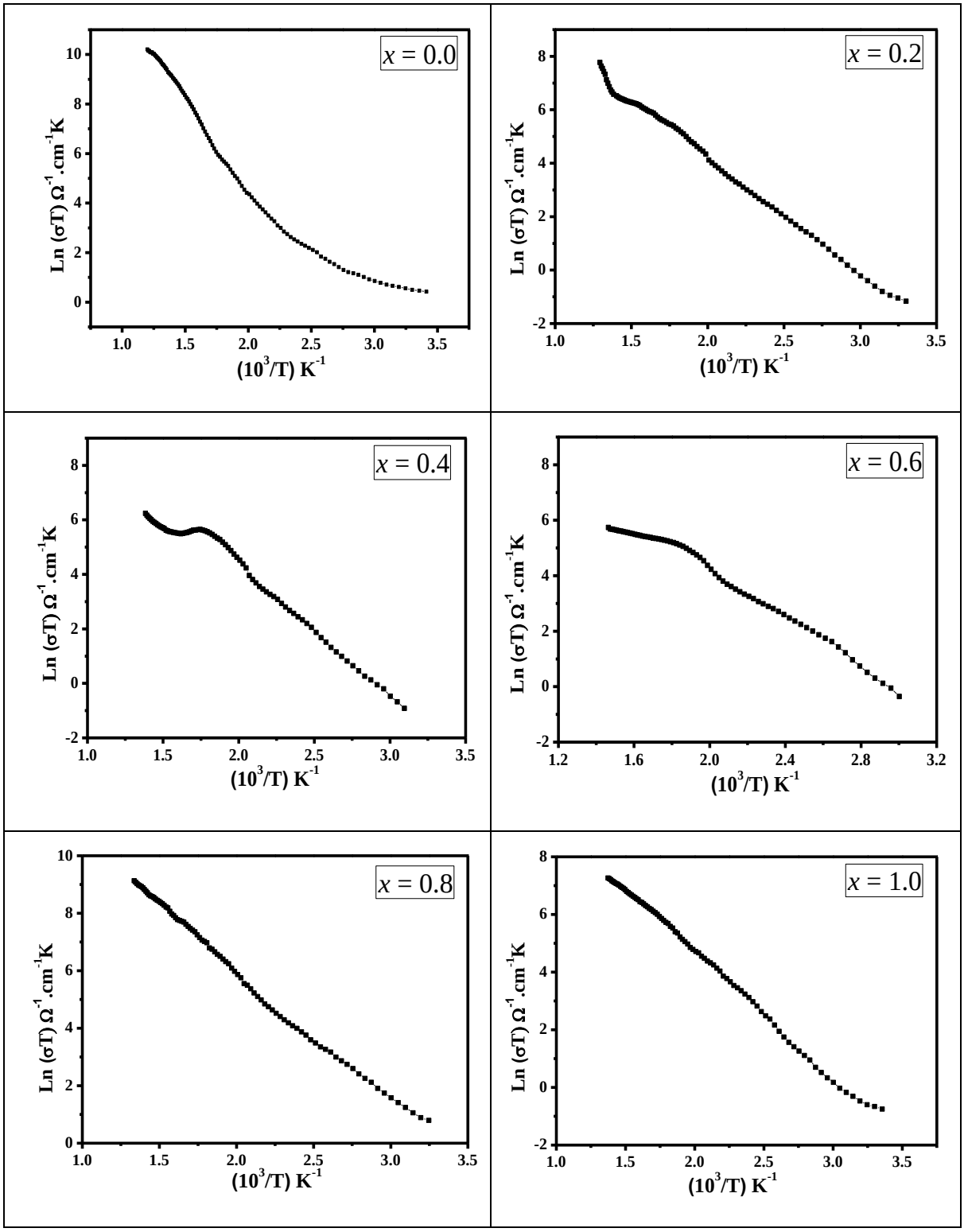

Figure (4.11): Variation of $\ln \sigma T$ with ($10^3/T$) for the samples with x = 0.0, 0.2, 0.4, 0.6, 0.8 and 1.0

4.3 Dielectric Properties

Dielectric properties such as dielectric constant (ε) and dielectric loss tangent ($\tan\delta$) are studied as a function of the applied frequency (υ) in the range of 10^4–$10^6 Hz$ at room temperature for the given mixed ***Li-Zn*** spinel ferrite.

The relation between ε and $\tan\delta$ with υ is given by the following equation (Lax and Button, 1962)

$$\varepsilon \tan(\delta) = \frac{\sigma_{AC}}{\upsilon} 1.8 \times 10^{10}$$

(4.12)

The above equation predicts that ε and $\tan\delta$ is inversely proportional to υ. The general trends for all compositions is that, ε and $\tan\delta$ are found to decrease continuously with increasing of υ and show normal dielectric behavior of the spinel ferrite. This behavior was, also, observed in various ferrite systems (Demirezen, 2013; El-Shaarawy, Rashad, Shash, Maklad and Afifi, 2015)

The variation of the ε verses υ is represented in figure (4.12). From this figure it is noticed that, the value of ε is decreased with increasing υ at low frequency region but at high frequency region, for *x*=0.0, 0.2 and 0.8, ε is slightly increased with increasing υ, while for *x*=0.4, 0.6 and 1, ε seems to be constant and independent of υ. The dielectric behaviour of ferrites can be explained on basis of dielectric polarization, which is found to be similar to that of conduction mechanism (Rahman, Sheaki, Pervin, Uddin, Ahmed, Abu Hossain, Rahman, Bashar, Hossain and Akhter, 2012).

The decrease in ε as υ increases may be due to electron exchange interaction between the Fe^{2+} and the Fe^{3+} ions, which cannot follow the alternating electric field. This behavior is because that the species contributing the polarizability are lagging behind the applied field at higher frequency (Farid, Ahmed, Aman, Kanwal, Murtaza, Ali, Ahmed and Ishfaq, 2015). The variation of ε with υ reveals the dispersion due to Maxwell Wagner type polarization, which is in agreement with Koop's Phenomenological theory (Rahman, Vargas and Ramana, 2014). The phenomenon of electron exchange between

Fe^{2+} and Fe^{3+} ions give rise to local displacement of charges in the direction of an applied electric field, which subsequently determines the polarization. The polarization decreases substantially with increase in υ and reaches a constant value due to the fact that beyond a certain υ of external field, the electron exchange between Fe^{2+} and Fe^{3+} ions cannot follow the alternating field (Ravinder, 1999; Cveji, Raki, Jankov, Skuban and Kapor 2009; Mansour, 2005; Mohan, Ravinder, Reddy and Boyanov, 1999).

At lower υ region both interfacial and dipolar polarization play their role whereas at high υ region only the electronic polarization contributes in hopping process. Moreover, the higher values of ε observed at lower υ, may be due to the predominance of species like Fe^{2+} ions, due to which interfacial dislocation piles-up oxygen vacancies and grain boundary defects…etc. A similar behavior was also observed at various ferrite systems (Demirezen, 2013; El-Shaarawy, et al 2015).

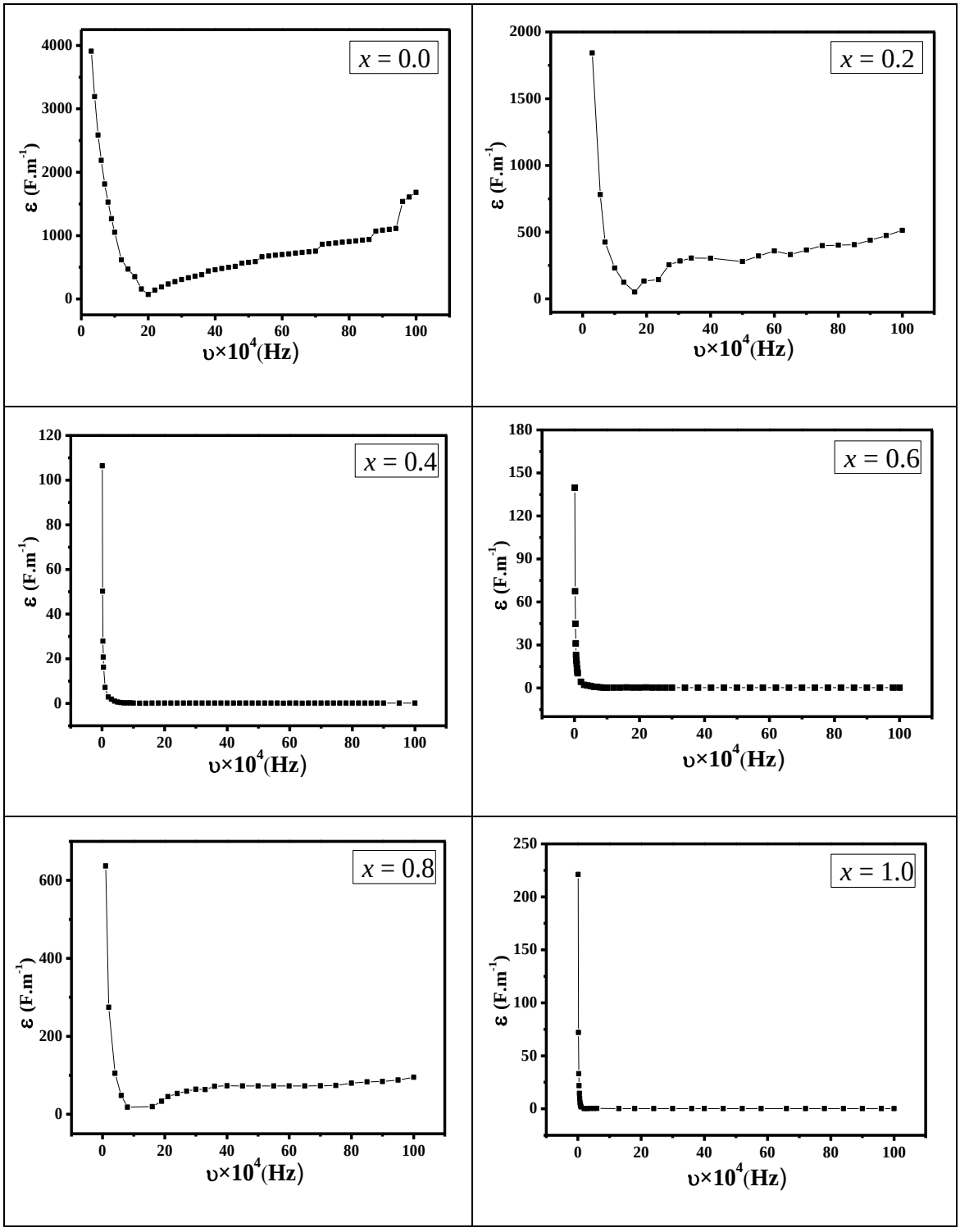

Figure (4.12): Variation of ε with υ for the samples with x = 0.0, 0.2, 0.4, 0.6, 0.8 and 1.0 at room temperature.

The variation of $\tan\delta$ with υ are shown in figures (4.13 a and b). These figures show that $\tan\delta$ has a maximum value (peak values) in frequency range of (2–20)×10^4 Hz. The peak values are found to shift towards lower frequency with increasing the content of $\boldsymbol{Zn^{2+}}$ ions. The peak values for the samples $Li_{0.5}Fe_{2.5}O_4$, $Li_{0.4}Zn_{0.2}Fe_{2.4}O_4$, $Li_{0.3}Zn_{0.4}Fe_{2.3}O_4$, $Li_{0.2}Zn_{0.6}Fe_{2.2}O_4$, $Li_{0.1}Zn_{0.8}Fe_{2.1}O_4$ and $ZnFe_2O_4$ were found at frequency of 20×10^4, 15.3×10^4, 12×10^4, 10×10^4, 8×10^4 and 2×10^4 Hz respectivly.

Aqualive explanation can be given for accurance of the maximum in the $\tan\delta$ versus υ curves in the case of mixed ***Li-Zn*** spinel ferrite. As pointed by Iwauchi (Iwauchi, 1971), there is a strong correlation between the conduction mechanism and dielectric behavior of ferites. The conduction mechanism in n-type ferrite is considered as due to hopping of electrons between $\boldsymbol{Fe^{2+}}$ and $\boldsymbol{Fe^{3+}}$. As such, when the hopping frequency is nearly equal to that of externally applied electric field, a maximum of loss tangent may be observed. In the case of samples of the mixed ***Li-Zn*** spinel ferrite of $x \geq 0.0$ aloss maximum are observed at (20, 15.3, 12, 10, 8 and 2)×10^4 Hz, respectively, as shown in figure(13.b). The condition for observing a maximumin the losses of a dielectric material is given by

$$\omega'\tau = 1 \tag{4-13}$$

where $\omega' = 2\pi\upsilon_{max}$ which is defined as the jumping probability per unit time, i.e. hopping probability (P),and τ is the relaxation time which is related to P by the relation $\tau = 1/2P$ then

$$\upsilon_{max.} \propto P \tag{4-14}$$

this mean that υ_{max} is proportional to P. Now a decrease of υ_{max} with increasing of $\boldsymbol{Zn^{2+}}$ ions indicates that the hopping probability per unit time is decrease continuously. This behavior was, also, observed in various ferrite systems (Krishna et al, 2012; Xavier, Thankachan, Jacob and Mohammed, 2015).

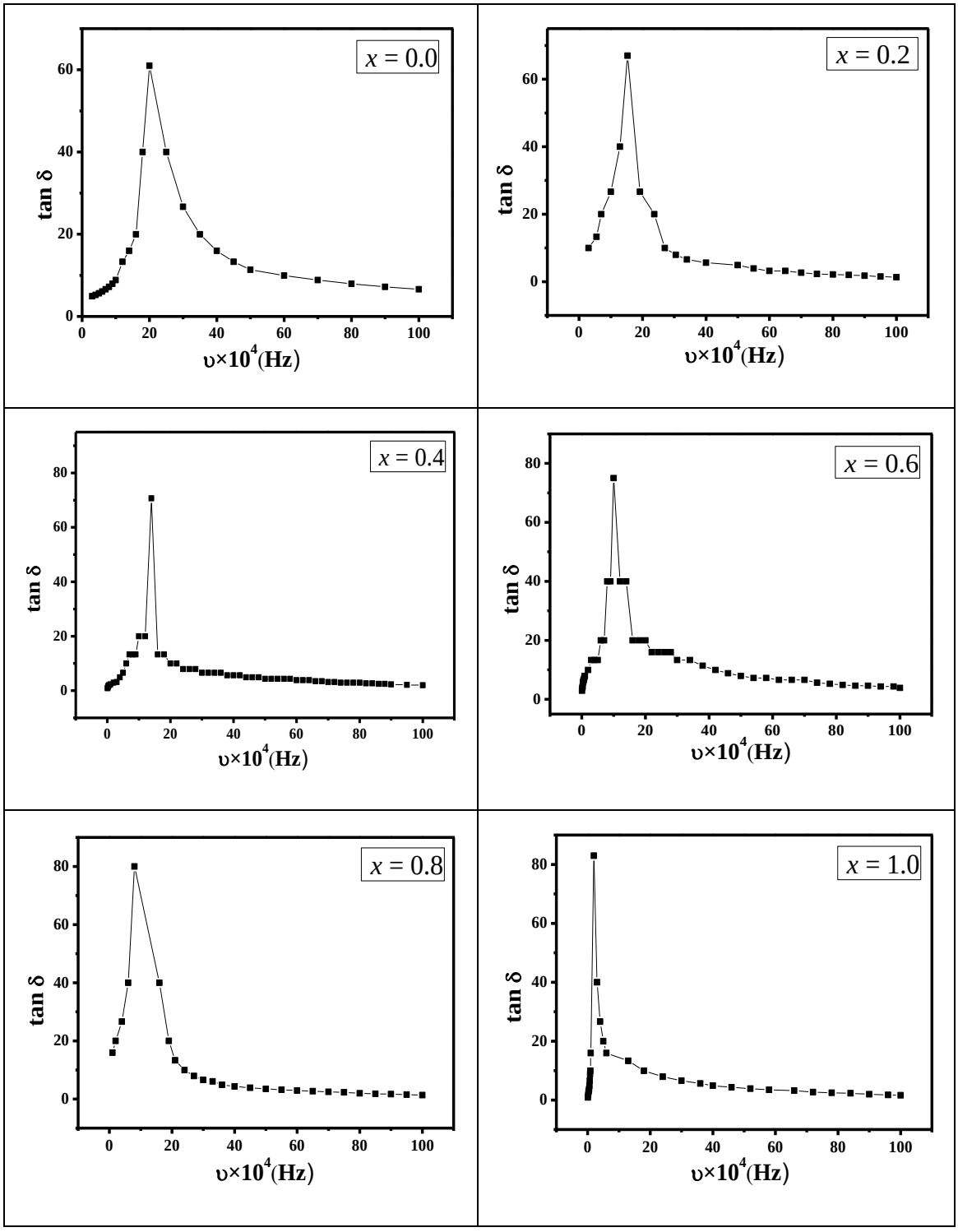

Figure (4.13 a): Variation of $\tan\delta$ with the υ for the samples with x = 0.0, 0.2, 0.4, 0.6, 0.8 and 1.0 at room temperature.

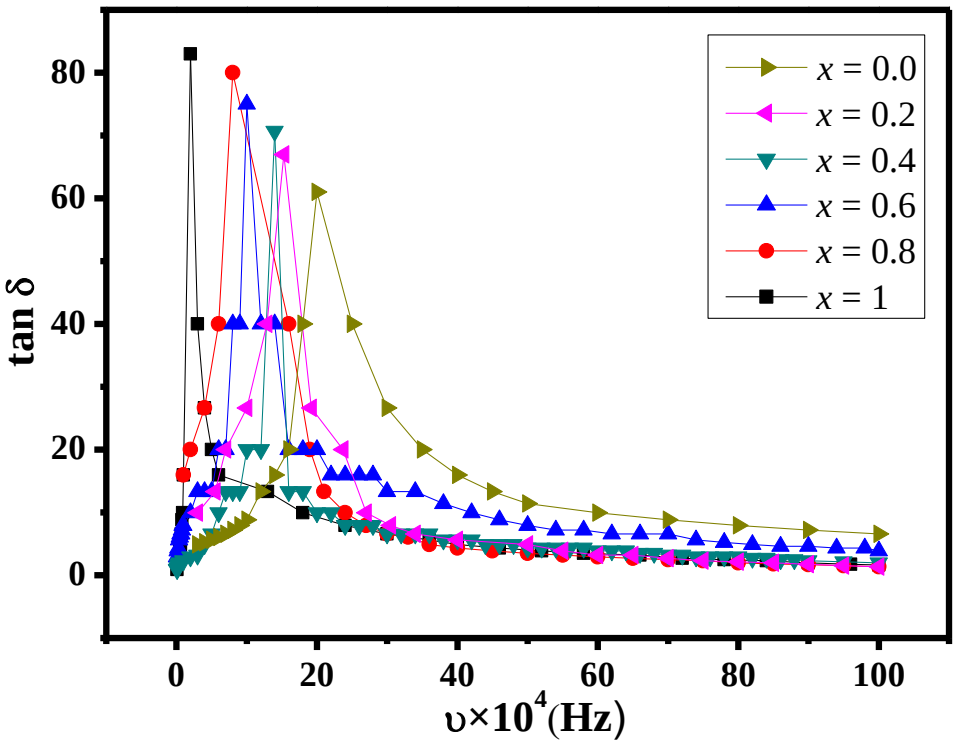

Figure (4.13 b): Variation of $\tan\delta$ with the υ for all samples at room temperature.

4.4 AC Conductivity

AC conductivity (σ_{AC}) has been investigated, at room temperature, in the frequency range of (10^4–10^6) *Hz* for the given mixed ***Li-Zn*** spinel ferrite. The expression for the σ_{AC} can be described in the form (Lax and Button, 1962)

$$\sigma_{AC} = \upsilon \frac{\varepsilon \tan\delta}{1.8\text{X}10^{10}} \Omega^{-1} m^{-1} \tag{4.15}$$

From the equation (4.15), it is clear that, σ_{AC} is directly proportional to υ; therefore, σ_{AC} is increased with increasing of υ as expected. The variation of σ_{AC} verses υ is represented in figure (4.14). As shown in this figure, σ_{AC} is increased with increasing of υ up to certain point then it seems to be constant and independent of υ. This agreed well with results obtained for many ferrite systems (Melagiriyappa, Veena, Somashekarappa, Shankaramurthy and Jayanna, 2014; Rani, Kumar, Batoo and Singh, 2014; Umapathy, Senguttuvan, Berchmans, Sivakumar, 2016).

The increase of σ_{AC} with increasing υ may be attributed to the dipole polarization i.e., the rotation of dipoles between two equivalent equilibrium positions is involved. It is the spontaneous alignment of dipoles in one of the equilibrium positions that give rise to the nonlinear polarization behavior of this composition (Noorkhan and Kalayne, 2012). The increment in σ_{AC} with υ has been explained by **Koop's** theorem (Koop, 1951), which supposed that the ferrites compact acts as multilayer capacitor. Both Maxwell–Wagner model and Koop's phenomenological theory reveal that ferrite materials consist of conducting grains separated by resistive thin layers of grain boundaries. As conduction processes is related to the dielectric polarization so almost a plane and similar region is observed for all samples due to affected grain boundaries with high resistance at low frequency region. On the other hand, at higher frequency region, grain effect and increasing trend of hopping of charge carriers Fe^{2+} - Fe^{3+} at adjacent O_h sites play a vital role thereby increasing conductivity (Reddy and Reddy, 1991).

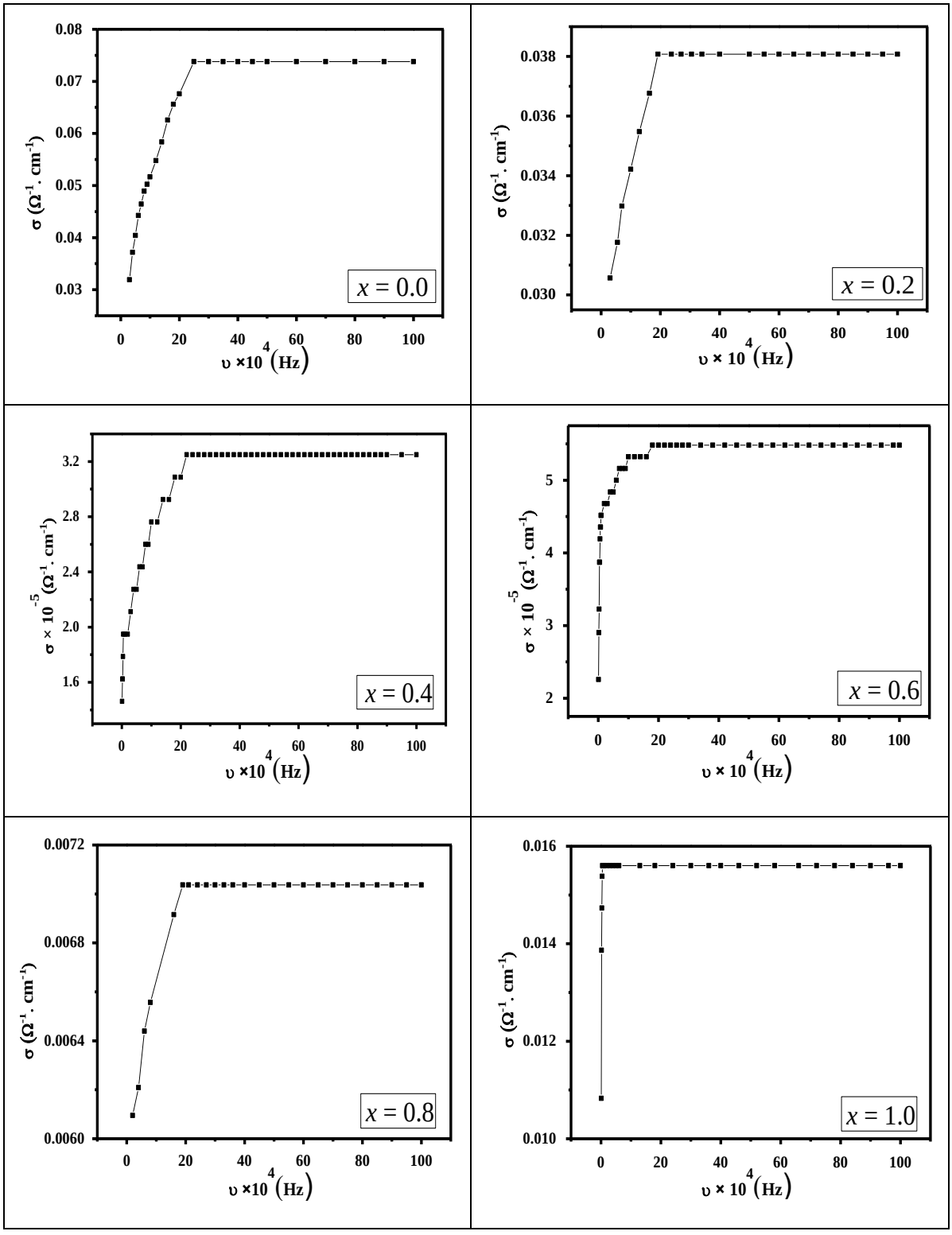

Figure (4.14): Variation of σ_{AC} against υ for the samples with x = 0.0, 0.2, 0.4, 0.6, 0.8 and 1.0 at room temperature.

Conclusion

Conclusion

Substitution of the non-magnetic Zn^{2+} ions in ***Li*** spinel ferrite has a tremendous influence such the magnetic, the electric and the dielectric properties. From this study, we concluded that:

- The μ_{net} in the spinel structure and the magnetic moments of T_d and O_h sites, μ_T and μ_O respectively are changed as increasing of Zn^{2+} ions.
- The ionic radii of T_d and O_h sites are found to change linearly with increasing of the Zn^{2+} ions.
- The magnetization increased with increasing of the Zn^{2+} ions for the samples with x= 0.0 up to x =0.6, but for samples of $x \geq 0.8$ have no magnetization.
- T_C decreases with increasing of Zn^{2+} content, and it is found that transition occurs for all samples except the samples with x = 0.8 and 1.0 which have no transition, so it is considered as a paramagnetic at room temperature.
- The transition temperatures obtained from DC conductivity measurement is in a good agree with that obtained from induction measurements.
- The activation energy in paramagnetic region is higher than in ferrimagnetic region.
- With increasing of the applied frequency, for all samples, it is found that dielectric constant decrease, but AC conductivity increase.
- From experimental results of dielectric loss tangent, maxima are occurred at certain frequency, and it is found to be shifted to lower frequency with increasing Zn^{2+} content.

Furthermore, Zn^{2+} content has significant influence on the electromagnetic properties, such as dielectric constant, dielectric loss tangent, electrical properties and magnetic properties for ***Li*** ferrites, so, the mixed ***Li-Zn*** spinel ferrite is considered a soft ferrite material, which is proved to be an interest material for technological and scientific applications.

References

References

Akhtar, M. N., Yahya, N. & Hussain, P. B. (2009). Structural and Magnetic Characterizations of Nano Structured $Ni_{0.8}Zn_{0.2}Fe_2O_4$ Prepared by Self-Combustion Method. *Inter. J. of basic and applied Sciences*, *9*(9), 37-40.

Albers, E. S. (1954). Ferrites for Microwave Circuits and Digital Computers. *J. Appl. Phys.*, *25*, 152.

Alone, S. T. & Jadhav, K. M. (2008). Structural and magnetic properties of zinc- and aluminum-substituted cobalt ferrite prepared by co-precipitation method. *Pramana-J Phys*, *70*(1), 173-181.

Anton, H. (1984). *Calculus with Analysis Geometry*. United States: John Wiley and Sons.

Aravind, G., Raghasudha, M. & Ravinder, D. (2015). Electrical transport properties of nano crystalline Li–Ni ferrites. *J. of Materiomics*, *1*(4), 348-356.

Belled, S. S., Pujar, R. B. & Chougule, B. K. (1998). Structural and Magnetic Properties of Some Mixed Li-Cd Ferrites. *Mat. Chem. Phys*, *52*(2), 166-169.

Blechstein, E. (1938). *Z. Physik.*, *39*, 212.

Cheng, H., (1984). Modeling of electrical response for semiconducting ferrite. *J. Appl. Phys.*, *56*(6), 1831.

Chikazumi, S. (1964). *Physics of Magnetism.* New York: John Wiley and Sons. Inc.

Chinnassamy, C. N., Narayanaasmy, A., Poupandian, N. & Chattopadhyay, K. (2001). The influence of Fe^{3+} ions at tetrahedral sites on the magnetic properties of nanocrystalline $ZnFe_2O_4$. *Mat. Sci. Eng. A*, *304-306*, 983-987.

Collectt, L. S. & Katsubel, T. S. (1973). Electrical Parameters of Rock in Developing Geophysical Techniques. *Geophysics*, *38*(1), 76-91.

Crangle, J. (1991). *Solid State Magnetism*. London: Edward Arnold.

Cveji, Z., Raki, S., Jankov, S., Skuban, S., Kapor, A. (2009). Dielectric properties and conductivity of zinc ferrite and zinc ferrite doped with yttrium. *J. Alloys and Compounds*, *480*, 241-245.

Dawoud, H. & Shaat, S. (2006). Magnetic Properties of Zn Substituted Cu Ferrite. *Al - Najah Univ. J. Res. (N. Sc.), 20*, 87-100.

Dawoud, H. A. & Shaat, S. K. K. (2006). Initial Permeability and DC Conductivity of Cu–Zn Ferrite. *J. of Series of Natural Studies and Engineering*, *14*(1), 165-182.

Dawoud, H. A. (1997). *A study of Some Electric and Magnetic Properties of Li-Cu Spinel*, Pd.D. Thesis, Faculty of Science Zagazig University, Egypt.

Demirezen, S. (2013). Frequency-and voltage-dependent dielectric properties and electrical conductivity of Au/PVA (Bi-doped)/n-Si Schottky barrier diodes at room temperature. *Appl. Phys. A, 112*(4), 827–833.

Dugdal, J. S. (1977). *The Electric Properties of Metals and Alloys*. London: Edward Arnold.

Eatah, A., Ghani, A. A., & Faramawy, E. (1988). Effect of sintering temperature on theelectrical conductivity and thermoelectric power of $CuFe_20_4$. *Phys. Stat. Sol*., *105*, 231-233.

El-Shaarawy, M. G., Rashad, M. M., Shash, N. M., Maklad, M. H. & Afifi, F. A. (2015). Structural, AC conductivity, dielectric behavior and magnetic properties of Mg-substituted $LiFe_5O_8$ powders synthesized by sol-gel auto-combustion method. *J. of Materials Science, Materials in Electronics, 26*(8), 6040–6050.

Farid, M. T., Ahmed, I., Aman, S., Kanwal, M., Murtaza, G., Ali, I., Ahmed, I., Ishfaq, M. (2015). SEM, FTIR and dielectric properties of cobalt substituted spinel ferrites. *J. of Ovonic Research*, *11*(1), 1-10.

Ferroxcube, (Jan. 2002). *Soft Ferrite*.

Gorter, E. W. (1954). Saturation magnetization and crystal chemistry of ferrimagnetic oxides. *Philips Res. Rept, 9*, 295.

Heikes, R. R. & Johnston, W. D. (1957). Mechanism of Conduction in Li-Substituted Transition Metal Oxides. *J. Chem. and Phys.*, *26*, 582.

Ishaque, M., Islam, M.U., Azhar Khan, M., Rahman, I.Z., Genson, A. & Hampshire S. (2010). Structural, electrical and dielectric properties of yttrium substituted nickel ferrites. *Physica B, 405*(6), 1532-1540.

Iwauchi, K. (1971). Dielectric properties of fine particles of Fe_3O_4 and some ferrites. *Jap J Appl Phys, 10*(11), 1520

Jacob, B.P., Thankachan, S., Xavier, Sh. (2013). Effect of Tb^{3+} substitution on structural, electrical and magnetic properties of sol–gel synthesized nanocrystalline nickel ferrite. *J. Alloys. Compd.*, *578*, 314-319.

Jadhav, P.A., Devan, R.S., Kolekar, Y.D. & Chougule, B.K. (2009). Structural, electrical and magnetic characterizations of Ni–Cu–Zn ferrite synthesized by citrate precursor method. *J. Phys. Chem. Sol*., *70*(2), 396-400.

Jebeli, M. Sh. & Mohamed, N.M.B. (2013). Synthesis and Characterization of Ni-Zn Ferrite Based Nanoparticles by Sol-Gel Technique. *International Journal of Material Science Innovations (IJMSI)*, *1*(1), 45-53.

Kittel, C. (1976). *Introduction to Solid State Physics*. (5^{th} Edition). United States: John Wily Sons.

Klinger M. I. (1977). Electron conduction in magnetite and ferrites1. *J. phys. Stat. sol. B*, *79*(1), 9-48.

Klinger. M. I. (1975). Two-Phase Polaron Model of Conduction in Magnetite-Like Solids, *J. of Phys. C: Solid State Physics*, *8*(21), 3595.

Koop, G. G. (1951). On the Dispersion of Resistivity and Dielectric Constant of Some Semiconductors at Audio frequencies. *Phys. Rev., 83*, 121.

Krishna, K. R., Kumar, K. V. & Ravinder, D. (2012). Structural and Electrical Conductivity Studies in Nickel-Zinc Ferrite. *J. of Advances in Materials Physics and Chemistry, 2*(3), 185-191.

Krishna, K. R., Ravinder, D., Kumar, K. V., Joshi, U. S., Rana, V. A. & Lincon, A. (2012). Dielectric Properties of Ni-Zn Ferrites Synthesized by Citrate Gel Method. *J. of Condensed Matter Physics, 2*(2), 57-60.

Kuanr, B. K., Singh, P. K., Kishan, P., Kumar, N., Rao, S. L. N., Sngh Prabhat K. & Sivastava, G. P. (1988). Dielectric and magnetic properties of polycrystalline cobalt-substituted LiTi ferrites. *J. Appl. Phys.*, *63*(8), 3780-3782.

Kulkarani, V. R., Todhar, M. M. & Vaingankar, A. S. (1986). Structural and Electrical Conductivity Studies in Nickel-Zinc Ferrite. *Ind. J. Pure Appl. Phys., 24*, 294.

Kumar, K. V., Sridhar, R., Ravinder, D. & Krishna, K. R. (2014). Structural properties and electrical conductivity of copper substituted nickel Nano ferrites. *J. of Applied Physics and Mathematics, 4*(2), 113-117.

Kumar, K.V. & Ravinder, D. (2001). Electrical transport properties of erbium substituted Ni–Zn ferrites. *Int. J. Inorganic Mater., 3*(7), 661-666.

Lax, B. & Button, K. J. (1962). *Microwave Ferrites and Ferrimagnetics*. New York: Mc. Grow-Hill.

Loders, K. & Fegley, B. (1998). *The Planetary Scientist's Companion*. New York: Oxford University Press

Lovell, M. C., Avery, A. J., Vernon, M. W. (1976). *Physical Properties of Materials.* New York: Van. Nostrand Reinhold Company.

Mansour, S. F. (2005). Frequency and composition dependence on the dielectric properties for Mg–Zn ferrite. *Egypt J. Solids*, *28*(2), 211-214.

Maria, K. H., Choudhury, SH. & Hakim, M.A. (2010). Complex Permeability and Transport Properties of Zn Substituted Cu Ferrites. *J. of Bangladesh Academy of Sciences, 34*(1), 1-8.

Mazen, S. A. (2000). Infrared absorption and dielectric properties of Li-Cu ferrite *Mat. Chem. and Phys., 62*(2), 139-147.

Mazen, S. A., Ghani, A. A. & Ashotr, A. H. (1985). Charge transport in Cu-Cd ferrospinels. *Phys. Stat. Sol.*, *88*, 343–346.

Melagiriyappa, E., Veena, M., Somashekarappa, A., Shankaramurthy, G. J. & Jayanna, H. S. (2014). Dielectric behavior and ac electrical conductivity in samarium substituted Mg–Ni ferrites. *Indian J. of Physics*, *88*(8), 795–801.

Mohan, G., Ravinder, D., Reddy, A.V. & Boyanov, B.S. (1999). Dielectric properties of polycrystalline mixed nickel–zinc ferrites. *Materials Letter, 40*(1), 39.

Moitgen, G., Angew, Z. (1952). *Phys. Rev*., *4*, 216.

Morrish, A. H. (1965). *The Physical Principles of Magnetism*. United States: John Wiley and Sons. Inc.

Nabiyouni, G., Fesharaki, M., Mozafari, M. & Amighian, J. (2010). Characterization and Magnetic Properties of Nickel Ferrite Nanoparticles Prepared by Ball Milling Technique. *J. Chin. Phys*., *27*, 126401.

Neel, L. (1948). Propriétés magnétiques des ferrites. Ferrimagnétisme et antiferromagnétisme. *Ann. Phys., 3*، 137-198.

Nwanje, J., *J. Phys*. (1980).

Noorkhan, P. A. & Kalayne, S. (2012). Synthesis, Characterization Ac Conductivity Of Nickel Ferrite. *I. J. of Engineering Research and Applications*, *2*(4), 681-685.

Patil, B. L., Sawant, S. R., Patil, S. A. & Patil, R. N. (1994). Electrical properties of Si^{4+} substituted copper ferrite. *J. Mat. Sci., 29*, 175-178.

Peloschek, H. P. (1963). *Square Loop Ferrites and the Applications*. London: J. Birks and Hart Heywood and Co. Ltd.

Pissurlekar, V. J. (2015). Structural and Magnetic Properties of Zn-Ni Ferrite Synthesized by Precursor Method. *J. of Science and Research*, *4*(12), 453-456.

Potakova, V. A., Zverv, N. D. & Romanov, V. P. (1972). On the cation distribution in $Ni_{1-x-y}FeZn_yFeO_4$ spinel ferrites. *Phys. Stat. Sol. (A), 12*(2), 623-627.

Putnis, A. (1992). *Introduction to mineral sciences*, United Kingdom: The Press syndicate of Cambridge University.

Rahman, M. M., Sheaki, Md., Pervin, S., Uddin, N., Ahmed, F., Abu Hossain, Md., Rahman, M., Bashar, M., Hossain, T. & Akhter, SH. (2012). Composition, Temperature and Frequency Dependent Magnetic, Dielectric and Electrical Properties of Magnesium-Zinc Ferrites. *J. of Bangladesh Academy of Sciences*, *36*(2), 199-212.

Rahman, Md. T., Vargas, M. & Ramana, C.V. (2014). Structural characteristics, electrical conduction and dielectric properties of gadolinium substituted cobalt ferrite. *J. of Alloys and Compounds, 617,* 547-562.

Rahman, S. A., Agami, W. R. & Eltabey, M. M. (2012). Frequency, Temperature and Composition Dependence of Dielectric Properties of Nd^{3+} Substituted Cu-Zn Ferrites. *J. of Life Science, 9*(4), 1630-1634.

Rani, R., Kumar, G., Batoo, Kh. & Singh, M. (2014). Influence of temperature on the electric, dielectric and AC conductivity properties of nano-crystalline zinc substituted cobalt ferrite synthesized by solution combustion technique. *Appl. Phys. A, 115*(4), 1401-1407.

Raut, A. V., Khirade, P. P., Humbe, A., Jadhav, S. A. & Shengule, D. R. (2016). *J. of Superconductivity and Novel Magnetism, 29*(5), 1331–1337.

Ravinder, D. & Latha, K. (1999). Dielectric behaviour of Mg-Zn ferrites at low frequencies. *Mat. Lett., 41,* 247-253.

Ravinder, D. (1999). Far-Infrared spectral studies of Mixed Lithium-Zinc ferrites *Mat. Lett., 40,* 205-208.

Ravinder, D. (2000). Electrical transport properties of Cadmium substituted Copper ferrites. *Mat. Lett., 43,* 129-138.

Raviner, D. & Kumar, K. (2001). Dielectric behaviour of erbium substituted Mn-Zn ferrites. *Bull. Mate. Sci., 24,* 505-509.

Reddy, M. B. & Reddy, P. V. (1991). Low-frequency dielectric behaviour of mixed Li-Ti ferrites. *J. Phys. D: Appl. Phys., 24,* 975-981.

Rezlesus, N. & Rezlesus, E. (1974). Dielectric Properties of. Copper Containing Ferrites. *Phys. Stat. Sol., 23*(2), 575-582.

Rudden, M. N. & Wilson, J. (1984). *Elements of Solid State Physics*. United States: John Wiley and Sons.

Sattar, A. A., El-Sayed, H. M. & Agami, W.R. (2007). Physical and Magnetic Properties of Calcium-Substituted Li-Zn Ferrite. *JMEPEG, 16,* 573–577.

Sattar, A. A., Wafik, A. H., El-Shokrofy, K. M. & El-Tabby M. M. (1999). Magnetic Properties of Cu–Zn Ferrites Doped with Rare Earth Oxides. *Phys. Solid Sta., 171*(2), 563.

Serway, R. A. (1996). *Physics For Scientists and Engineers with Modern Physics (6th ed.)* Philadelphia: Saunders College Publishing.

Shaat, S. K. K. (2012). *Advanced Ferrite Technology*. LAMBART.

Shinde, T.J., Gadkari, A.B. & Vasambekar, P.N. (2013). Magnetic properties and cation distribution study of nanocrystalline Ni–Zn ferrites. *J. of Magnetism and Magnetic Materials, 333*, 152–155.

Shinde, U. B., Shirsath, S. E., Patange, S. M., Jadhav, S. P., Jadhav, K. M. & Patil, V. L. (2013). Preparation and characterization of Co^{2+} substituted Li–Dy ferrite ceramics. *Ceramics International, 39*(5), 5227-5234.

Smit, J. & Wijn, H. P. J. (1959). *Ferrites*, New York: John Wiley.

Snelling, E. C. (1964). *Proc. Brit. Ceramic Soc. Z., 2*, 151.

Snelling, E. C. (1969). *Soft Ferrites Properties and Applications*, London: IIIFFE.

Snoek, J. L. (1947). *New Developments in Ferromagnetic Materials*. New York-Amsterdam: Elsevier Publishing Co., Inc.

Standly, K. J. (1972). *Oxide Magnetic Materials*. United Kingdom: Clarendon Press.

Tang, X., Manthiram, A. & Goodenough J. B. (1989). Copper ferrite revisited. *J. Sol. State Chem., 79*(2), 250-262.

Tareev, B. (1975). *Physics of Dielectric Materials*. Moscow: C.M. Publishers.

Tayal, D. C. (1998). *Electricity and Magnetism.* Himalaya Publishing House.

Uitert, L. G. (1956). Dielectric Properties of and Conductivity in Ferrites. *J. of Chem. and Phys., 24*,1294-1303.

Umapathy, G., Senguttuvan, G., John Berchmans, L. & Sivakumar V. (2016). Structural, dielectric and AC conductivity studies of Zn substituted nickel ferrites prepared by combustion technique. *J. of Materials Science, 27*(7), 7062–7072.

Upadhyay, C., Verma, H. C., Rath, C., Sahu, K. K., Anand, S., Das, R. P. & Mishra, N. C. (2001). Mössbauer studies of nanosize $Mn_{1-x}Zn_xFe_2O_4$. *J. of Alloys and Compounds*, *326*(1), 94-97.

Verwey, E. J. W. & Helimann, E. L. (1947). Physical Properties and Cation Arrangement of Oxides with Spinel Structures I. Cation Arrangement in Spinels. *J. Chem. Phys., 15*, 174.

Verwey, E. J. W., Deboer, F. & Vansanten, J. H. (1948). Cation Arrangement in Spinels. *J. Chem. Phys, 16*, 12.

Vishwanathan, B. & Murthy, V. R. K. (1990). *Ferrites Materials: Sci. Technol.* Mumbai: Narosa Publishing House.

Xavier, S., Thankachan, S., Jacob, B. P. & Mohammed, E. M. (2015). Structural and electrical properties of neodymium substituted cobalt ferrite nanoparticles. *IOP Conf. Series: Materials Science and Engineering, 73*, 012093.